Understanding each other's models: a standard representation of global water models to support improvement, intercomparison, and communication

Camelia-Eliza Telteu[1], Hannes Müller Schmied[1,2], Wim Thiery[3], Guoyong Leng[4], Peter Burek[5], Xingcai Liu[4], Julien Eric Stanislas Boulange[6], Lauren Seaby Andersen[7], Manolis Grillakis[8], Simon Newland Gosling[9], Yusuke Satoh[6], Oldrich Rakovec[10,11], Tobias Stacke[12], Jinfeng Chang[13,14], Niko Wanders[15], Harsh Lovekumar Shah[16], Tim Trautmann[1], Ganquan Mao[17], Naota Hanasaki[6], Aristeidis Koutroulis[18], Yadu Pokhrel[19], Luis Samaniego[10], Yoshihide Wada[5], Vimal Mishra[16], Junguo Liu[17], Petra Döll[1, 2], Fang Zhao[20], Anne Gädeke[7], Sam Rabin[21], Florian Herz[1]

[1]Institute of Physical Geography, Johann Wolfgang Goethe University Frankfurt, Frankfurt am Main, 60438, Germany
[2]Senckenberg Leibniz Biodiversity and Climate Research Centre (SBiK-F), Frankfurt am Main, 60325, Germany
[3]Department of Hydrology and Hydraulic Engineering, Vrije Universiteit Brussel, Brussels, 1050, Belgium
[4]Key Laboratory of Water Cycle and Related Land Surface Processes, Institute of Geographic Sciences and Natural Resources Research, Chinese Academy of Sciences, Beijing, 100101, China
[5]International Institute for Applied Systems Analysis, Laxenburg, 2361, Austria
[6]National Institute for Environmental Studies, Tsukuba, 305–8506, Japan
[7]Potsdam Institute for Climate Impact Research, Potsdam, 14473, Germany
[8]Institute for Mediterranean Studies, Foundation for Research and Technology-Hellas, Rethymno, 74100, Greece
[9]School of Geography, University of Nottingham, Nottingham, NG7 2RD, United Kingdom of Great Britain and Northern Ireland
[10]Department Computational Hydrosystems, UFZ-Helmholtz Centre for Environmental Research, Leipzig, 04318, Germany
[11]Faculty of Environmental Sciences, Czech University of Life Sciences Prague, Prague, 16500, Czech Republic
[12]Institute of Coastal Research, Helmholtz-Zentrum Geesthacht, Geesthacht, 21502, Germany
[13]College of Environmental and Resource Sciences, Zhejiang University, Hangzhou, 310058, China
[14]Laboratoire des Sciences du Climat et de l'Environnement, CEA-CNRS-UVSQ/IPSL, Université Paris Saclay, Gif sur Yvette, 91191, France
[15]Department of Physical Geography, Utrecht University, Utrecht, 3508, The Netherlands
[16]Indian Institute of Technology Gandhinagar, Palaj, Gandhinagar, 382355, India
[17]School of Environmental Science and Engineering, Southern University of Science and Technology, Shenzhen, 518055, China
[18]School of Environmental Engineering, Technical University of Crete, Chania, 73100, Greece
[19]Department of Civil and Environmental Engineering, Michigan State University, East Lansing, Michigan, 48824, United States of America
[20]School of Geographic Sciences, East China Normal University, Shanghai, 200241, China
[21]Karlsruhe Institute of Technology, Institute of Meteorology and Climate Research / Atmospheric Environmental Research, Garmisch-Partenkirchen, 82467, Germany

Correspondence to: Camelia-Eliza Telteu (telteu@em.uni-frankfurt.de, camelia.telteu@gmail.com)

Abstract. Global water models (GWMs) simulate the terrestrial water cycle, on the global scale, and are used to assess the impacts of climate change on freshwater systems. GWMs are developed within different modeling frameworks and consider different underlying hydrological processes, leading to varied model structures. Furthermore, the equations used to describe various processes take different forms and are generally accessible only from within the individual model codes. These factors

have hindered a holistic and detailed understanding of how different models operate, yet such an understanding is crucial for explaining the results of model evaluation studies, understanding inter-model differences in their simulations, and identifying areas for future model development. This study provides a comprehensive overview of how state-of-the-art GWMs are designed. We analyze water storage compartments, water flows, and human water use sectors included in 16 GWMs that provide simulations for the Inter-Sectoral Impact Model Intercomparison Project phase 2b (ISIMIP2b). We develop a standard writing style for the model equations to further enhance model improvement, intercomparison, and communication. In this study, WaterGAP2 used the highest number of water storage compartments, 11, and CWatM used 10 compartments. Seven models used six compartments, while three models (JULES-W1, Mac-PDM.20, and VIC) used the lowest number, three compartments. WaterGAP2 simulates five human water use sectors, while four models (CLM4.5, CLM5.0, LPJmL, and MPI-HM) simulate only water used by humans for the irrigation sector. We conclude that even though hydrologic processes are often based on similar equations, in the end, these equations have been adjusted or have used different values for specific parameters or specific variables. Our results highlight that the predictive uncertainty of GWMs can be reduced through improvements of the existing hydrologic processes, implementation of new processes in the models, and high-quality input data.

1 Introduction

Many multi-model intercomparison projects (MIPs) have been designed to provide insights into various Earth system processes. Some MIPs examples include FireMIP for the fire regime and its drivers (Rabin et al., 2017); CMIP for past, present, and future climate changes and their drivers (Eyring et al., 2016; Kageyama et al., 2018); LakeMIP for physical and biogeochemical processes of lakes (Stepanenko et al., 2010; Thiery et al., 2014); AgMIP for crop growth (Rosenzweig et al., 2013), and WaterMIP or ISIMIP for the water cycle (Haddeland et al., 2011; Frieler et al., 2017). These MIPs provided many multi-model ensembles that consist of multiple models driven by the output of multiple other models. The multi-model ensembles offer the opportunity to inter-compare models for an increased understanding of process representation and inter-model differences as well as for model improvement. Hence, they have evaluated models' performance in the past and have focused on the models' agreement for the future. They also have encountered many challenges in how to inter-compare models and interpret various model results (Von Lampe et al., 2013), realize the standardization of data and scenarios, and integrate transdisciplinary knowledge in modeling (Rosenzweig et al., 2013), identify and reduce uncertainties (Sitch et al., 2008). In the end, many MIPs and their multi-model ensembles have been blocked in interpreting inter-model differences (Clark et al., 2011). They have underlined the need to go beyond good overall model performance and to improve process representation in the models (Guseva et al., 2020), integrate missing processes (Friend et al., 2013) and reduce uncertainties (Warszawski et al. 2013). Certainly, MIPs have also been affected by scientific complexity, input data quality, and technical infrastructure. Therefore, the modeling community is still testing and learning how to improve modeling and how to realize multi-model inter-comparison studies. For example, the Coupled Model Intercomparison Project (CMIP) adopted, after 20 years of existence, a new and more federated structure because of complex scientific questions, large amount of model outputs, challenges of technical infrastructure, and even cultural and organizational challenges (Eyring et al., 2016). CMIP also showed that robust similarities exist among models and, as a result, models are not strictly independent of each other given previous and legacy versions, and existing links among modeling communities who indirectly transfer some models' strengths and weaknesses by sharing their ideas and codes (Masson and Knutti, 2011; Knutti et al., 2013). Finally, few studies have

undertaken model experiments on process representation and evaluated the models for specific events or characteristics
80   specifically on the catchment scale (Boer-Euser et al., 2017; Duethmann et al., 2020). It has been concluded that there is no
perfect model (Essery et al., 2013; Ullrich et al., 2017) and there is a need to understand better how models work.

Therefore, in this complex scientific context, the present study represents a step forward towards an increased understanding
of process representation and inter-model differences. The three main goals are (i) to provide a better understanding of how
state-of-the-art global water models are designed, (ii) to show similarities and differences among them, based on their
85   equations, and (iii) to underline future research potential in global hydrological modeling.

This study supports intercomparison, improvement, and communication among models. It also provides the basis for 1. further
water model (inter)comparison studies, including model outputs; 2. selecting the right model(s) for a given application; and 3.
identifying data needs for a given analysis and application.

The target audience includes students, professors, the modeling community, the stakeholder community, and members of the
90   general public interested in understanding large-scale models, and simulating climate change and its impacts.

Hence, we present the modeling approaches in simulating globally terrestrial water cycle in section 2. In section 3, we present
key characteristics of the models included in the present study. In section 4, we review models and present their strengths and
weaknesses. In section 5, we present similarities and differences among models. In section 6, we discuss challenges and future
research potential in global hydrological modeling. In the end, we present our conclusions.

2. Modeling approaches in simulating terrestrial water cycle globally

The terrestrial water cycle is simulated globally by three different communities that have developed three types of models: (i)
the climate community has developed land surface models (LSMs); (ii) the global hydrological community has developed
global hydrological models (GHMs); (iii) the vegetation community has developed dynamic global vegetation models
(DGVMs). These communities interact with each other, but generally focus on specific hydrological processes that are
100   important for their research and are presented in the following subsections.

2.1 Differences in modeling approaches

The climate community is focused on climate simulations (long-term weather patterns in an area) and their changes over
decades and centuries. LSMs simulate the water and energy exchanges between the land surface and the atmosphere,
specifically focusing on vertical flow exchanges. Therefore, these models simulate the energy cycle, the water cycle, the carbon
105   and nitrogen cycles, and vegetation and crop responses to temperature, precipitation, and CO_2 concentrations. Further, they
represent the soil with a higher vertical resolution and represent evapotranspiration and snow dynamics in a more physical
manner than the global hydrological models (GHMs; Döll et al., 2016; Pokhrel et al., 2016; Wada et al., 2017). Ultimately,
they are fundamental components of global climate models (GCMs) and Earth system models (ESMs).

The global hydrological community is focused on surface hydrologic processes, primarily river flow simulation and its daily

110   to century-scale changes. GHMs simulate the water cycle with its water flows, water storage compartments, and human water use sectors. These models simulate water abstracted for the irrigation, domestic use, livestock, industry (manufacturing and electricity), and desalination sectors. One of their main foci is streamflow simulation and their ability to reproduce historical observations of this variable. They focus on lateral flows and only partly on vertical flows, comprehensively simulating the following surface water bodies: (i) lakes, (ii) wetlands, (iii) rivers.

115   The vegetation community is focused on vegetation distribution and growth in an area and over a time interval and is primarily interested in the global carbon cycle. DGVMs simulate shifting vegetation, driven by biogeochemistry, hydrology, and anthropogenic influences. These models simulate the vegetation composition and distribution as well as compartments and flows of carbon and water, for both natural and agricultural ecosystems. Specifically, they model the active response of vegetation to changes in air temperature, precipitation, and CO_2 concentrations.

120   The main driver that connects the processes simulated by these communities is solar energy, specifically, it links the water and energy budgets with vegetation processes. This can be exemplified by the latent heat flux of evaporation that describes the heat or the energy required to change the liquid water into water vapor. This heat or energy is locked in the humid air as water vapor, and is released when the humid air touches cold air and water vapor condensation starts. Therefore, continental evaporation is considered to be water loss by the global hydrological and vegetation modeling communities, but a water source

125   (for cloud formation) by the climate community (those that simulate the atmosphere), with implications for agriculture and ecosystems (Abbott et al., 2019). Additionally, transpiration represents a water source for the vegetation community, necessary for photosynthesis and plant growth, and water loss for the global hydrological community.

Although these communities simulate the same hydrological processes, they use the same expressions or terminology with different, field-specific meanings. Some examples are presented in subsection 2.2.

130   In conclusion, all these models simulate the water cycle at the global scale despite fundamental differences in model structure, model parameterization, and output variables.

2.2 Ambiguity of terminologies used in hydrological modeling

This subsection highlights the same expressions used by the three communities, but with different meanings. For example, *climate forcings* (factors) are used by climate community to point out the natural and human-made factors that affect the

135   Earth's climate. Natural factors include the Sun's energy, regular changes in the Earth's orbital cycle, and large volcanic eruptions, while human-made factors are greenhouse gas emissions and land use changes. The global hydrological community and vegetation community consider *climate forcings* as climate input data or climate variables for their models.

Another example is *dynamic vegetation*, which has two meanings among these communities: 1. *active vegetation* defines vegetation that actively changes in an area because of changes in the CO_2 concentration, that is CO_2 assimilation through plant

140   stomata in the photosynthesis process and because of changes in air temperature and precipitation; 2. *dynamic vegetation*, also called *vegetation competition*, defines vegetation that changes its geographical distribution from one geographical area to

another because of competitive and biogeographical processes determined by climate change (geographical distribution of plants) or human activities. In the present study, we use *active vegetation* to highlight if models include the photosynthesis scheme in their structure. Generally, it is recommended to include this process in models because elevated CO_2 concentrations

145 cause physiological and structural effects on plants and indirectly influence runoff and evapotranspiration over a geographical area. The physiological effect reduces the opening of leaf stomata because less water is needed to assimilate carbon, leading to decreased transpiration and, indirectly, increased runoff. The structural effect or fertilization effect causes an increase in plant growth and leads to increased transpiration per unit area and, indirectly, a decreased runoff (Gerten et al., 2014). However, Singh et al. (2020) demonstrated that increased leaf area under elevated CO_2 concentrations (structural effect) might

150 counterbalance the increased water use efficiency (physiological effect).

In the end, because of differing and complementary perceptions and details of their models, it is important that these communities interact, identify their similarities and differences, share experiences, learn from different experiments, undertake joint experiments, present and discuss their results, and discuss how they influence and depend on each other and how hydrological modeling can be improved. Therefore, collaboration among these communities will result in new multi-model

155 intercomparison projects and multi-model ensembles that will facilitate new analyses, comparisons, understandings, and improvements.

3 Global water models included in the study

3.1 Description of the modeling experiment

The GWMs analyzed in this study contribute with simulations to the Inter-Sectoral Impact Model Intercomparison Project

160 (ISIMIP). This project was initiated by the Potsdam Institute for Climate Impact Research (PIK) and the International Institute for Applied Systems Analysis (IIASA) in 2012. It includes a strategy and a framework to create, compare, and explain climate-impact projections in various sectors and at varying scales (Warszawski et al., 2014). ISIMIP has gone through various simulation phases (Fast Track, 2a/2b, currently 3a/3b), each designed with a specific focus topic that has dictated the protocol framework, including specific simulation scenarios and common input datasets. All models participating in ISIMIP have to

165 comply with its simulation protocol (Frieler et al., 2017). The ISIMIP project has been offering a forum where scientists from, currently, 13 sectors, including the global water sector, bring their expertise, experience, and knowledge together to extend the frontier of research on climate change and its cross-sectoral impact assessments. In its second phase (ISIMIP 2b), most models are run with a daily temporal resolution and with a spatial resolution of $0.5° \times 0.5°$ (~55 km × 55 km at the Equator). The models of the global water sector contribute to an experiment setup designed to assess the impact of historical and future

170 warming under the Paris Agreement. These models are driven by the same climate input datasets under representative concentration pathways (RCPs) and socioeconomic scenarios (SSPs). The time span of the simulations is divided into pre-industrial (1661–1860), historical (1861–2005) and future (RCP2.6, RCP6.0, and RCP8.5). The requested output datasets provide quantitative information to identify the major drivers of historical impacts, to examine the impacts of additional

warming, and to assess the impacts from different future socioeconomic development scenarios. More details regarding the
175 ISIMIP framework can be found on the ISIMIP webpage (https://www.isimip.org/) and in Frieler et al., 2017. However, one
recommendation for the ISIMIP community will be to increase the number of regional studies and pilot studies that could
validate global studies, which could be another effective way of studying climate change.

3.2 Steps taken to realize the standard writing style of model equations

All models that provide simulations for the global water sector in ISIMIP2b are included in this paper, although some of them
180 have not yet finished their simulations for this phase. The rationale of describing models is based on how models simulate the
water cycle. Therefore, in this study, a global water model describes the dynamic behavior of a hydrological system that
includes input variables, state variables, parameters, constants, and output variables (Bierkens and van Geer, 2007). State
variables define the state of the water in a compartment or storage at the beginning of the simulation, and can change in space
and time, for example, with canopy water storage. Their variation is caused by a variation of the input variables, for example,
185 precipitation. State variables are related to the input variables and output variables through parameters. Parameters may change
in space, but do not change in time. Parameters and coefficients represent numbers that describe a particular characteristic of
reality, of the model, of the catchment area or flow domain such as runoff coefficient, soil porosity, hydraulic conductivity of
different soil horizons, maximum soil water storage, maximum canopy water storage, and mean residence time in the saturated
zone (Beven, 2012). Some processes are parameterized, meaning that their values are precisely marked in the computer code
190 and are not calculated by the model itself. Originally, to parameterize by itself means to describe a process or a phenomenon
by the use of parameters. Therefore, in hydrological modeling many parameterization methods or techniques (equations
running in some algorithms) have been implemented to simulate hydrological processes. Ultimately, a model also uses
constants, properties of the model that do not change in space and time, and "output variables," which vary in space and time.
Hence, we describe GWMs based on the equations implemented for eight water storage compartments, five human water use
195 sectors, and desalination. The analyzed water storage compartments are (1) canopy, (2) snow, (3) soil, (4) groundwater, (5)
lake, (6) wetland, (7) reservoir, and (8) river. The human water use sectors are (1) irrigation, (2) domestic (households), (3)
livestock, (4) manufacturing, (5) electricity.

It was extremely challenging to label processes as being similar or different among the 16 models because a unique equation
can be implemented in various ways (e.g., discrete vs. analytical form, focusing on flows or water storage compartments) or
200 parameterized differently. Therefore, we created a standard writing style for GWMs equations and used the same symbols to
write those equations, thereby highlighting their similarities and differences in a consistent way. In the end, the standard writing
style facilitated comparison among models, but it has also raised many challenges, mainly because we decided to write self-
explanatory equations that could be understandable by readers with or without knowledge in hydrology.

In the supplement, we report tables containing various equations for each water storage compartment, human water use sector,
205 and their related water flows (tables and figures in the supplementary information are denoted by an "S" in their numbering).
All variables have been harmonized and their units have been standardized (Tables S1–S83).

We made the standard writing style of the model equations following some steps. Firstly, we analyzed the nomenclature of each model with the purpose of identifying the best practices. Secondly, we assembled a list with water storage compartments, flows, and human water use sectors included in the models. Thirdly, we established clear definitions for all variables that have
210 been collected inside a glossary of terms. Finally, we collated all model equations of each inflow and outflow for each water storage compartment and human water use sector.

Multiple subscripts or superscripts are required to properly identify water storage compartments, flows, and human water use sectors because of the large number of compartments that are included in the model structures. Thus, we selected "S" to describe water storage, "P" to describe everything connected to precipitation, "E" everything related to evaporation, "R"
215 everything related to runoff, "Q" everything related to streamflow and outflow, and "A" for water abstractions. We used two letters for subscripts and superscripts, ideally, the first two letters of the word, for example, "ca" for canopy; "sn" for snow; "so" for soil, and so on (see list of symbols and glossary in the Supplement), while we used the first letter of each word in case of compounds words such as groundwater ("gw") or surface water ("sw"). We separated subscripts and superscripts from one another using comma. Some of these decisions correspond with some habits that exist in the hydrological community (e.g., *gw*
220 and *sw*) and we decided to keep them to make a comfortable and easy workflow for modelers and readers. We did not write full words for subscripts and superscripts, because equations became too long and difficult to read and understand.

In the end, the standard writing style of the equations is useful and necessary for finding similarities and differences among models for each water storage, human water use sector, and water flow. In addition, it can be leveraged for explaining the different model outputs, for classification of the models based on cluster analysis, and for selecting the right model for the
225 right application. It can also be used for drawing a standard schematic visualization of the water cycle, for describing models on ISIMIP and ISIpedia platforms (the open climate-impacts encyclopedia, a part of the ISIMIP, https://www.isipedia.org/), and for understanding how models work. It should be noted that these equations are available only for model versions used for ISIMIP2b.

3.3 Key characteristics of the global water models

230 The present model intercomparison study is based on the lists presented in Tables 1 to 5 that show water storage compartments, flows, and use sectors included in the GWMs. Generally, the model description is separated into two parts: the hydrological part and human water use part. The hydrological part includes the water cycle processes described as water storage compartments and flows, with flow presented as inflow and outflow of each water storage, while the water use part includes human water use, specifically water abstracted from the groundwater or surface waters. In the supplement, we provide tables
235 that present an overview of the GWMs, helping readers to understand similarities and differences among models, identify included water storage and flows, and get an overview of hydrological knowledge complexity behind models (Tables S1–S103).

In this study, six models are LSMs: CLM4.5, CLM5.0, DBH, JULES-W1, MATSIRO, and ORCHIDEE. Nine models are GHMs: CWatM, H08, Mac-PD20, mHM, MPI-HM, PCR-GLOBWB, VIC, WaterGAP2, and WAYS. One model is a DGVM
240 (LPJmL, Tables 6 and 12).

Twelve models have a daily temporal resolution (Table 6), while MATSIRO has an hourly temporal resolution. Four models (CLM4.5, CLM5.0, MATSIRO, and ORCHIDEE) have 30-min temporal resolution, downscaling their daily forcing to a 30-min time step to solve the energy budget. JULES-W1 has a higher temporal resolution (1-hour) to solve the energy budget. Fifteen models run with a spatial resolution of 0.5°. ORCHIDEE runs with a spatial resolution of 1.0° and has its outputs
245 converted to 0.5° spatial resolution. All models divide the land into grids of discrete "cells" (excluding Greenland and Antarctica) and, in addition, some models include subgrids for some components: CLM4.5 and CLM5.0 for vegetation, surface runoff and evapotranspiration; H08 for land cover (via 19 crop types); CWatM for land cover (6 land cover types) and snow (10 elevation zones); MPI-HM for surface runoff and evapotranspiration; PCR-GLOBWB for vegetation and land cover; WaterGAP2 and MATSIRO for snow; VIC for vegetation and elevation. Further, MATSIRO divides a subgrid cell in snow-
250 covered and snow-free portions with flows and storages resolved separately for these portions, both for land and canopy surfaces.

Nine models (CLM4.5, CLM5.0, CWatM, H08, LPJmL, MATSIRO, MPI-HM, PCR-GLOBWB, WaterGAP2) use the 30-min global drainage direction map DDM30 (Döll and Lehner, 2002), a raster map with a spatial resolution of 0.5° × 0.5° (~ 50 km × 50 km), to outline the drainage directions of surface water collected by creeks, rivulets, and rivers. In this map, 66,896
255 discrete grid cells are connected to each other by their specific drainage direction and are organized into drainage basins that drain from the Earth's land surface (excluding Antarctica) into the ocean or into an inland sink. The mHM uses a river network (0.5° × 0.5°) upscaled from HydroSHEDS (Lehner et al., 2006). ORCHIDEE uses the river network from the Simulated Topological Networks (STN-30p: Vörösmarty et al., 2000). Five models (DBH, JULES-W1, Mac-PDM.20, VIC, and WAYS) do not use any river routing scheme for the ISIMIP2b; therefore, they do not compute streamflow.
260 MATSIRO and LPJmL use prescribed data for the domestic (household) and industry sectors; therefore, they do not consider the two-way interaction between water system and humans. In hydrological modeling and in the ISIMIP2b, the word "prescribed" has two meanings: (i) data which are simulated by other models and provided by the ISIMIP2b framework as input (https://www.isimip.org/gettingstarted/details/38/); (ii) data obtained from satellite observations, other datasets, or maps. Prescribed data highlight some limitations of the models or underline the lack of some processes that were intentionally or
265 non-intentional removed from the model structure, according to the purpose of the model development or other priorities such as time.

Six GHMs perform calibration of their hydrological components, using different approaches (Table 6). CWatM calibrates monthly or daily streamflow for 12 catchments using the Distributed Evolutionary Algorithms in Python (DEAP) approach (Burek et al., 2020), while WaterGAP2 uses a beta function for the calibration of 1,319 gauged hydrological stations
270 considering runoff as a nonlinear function of soil moisture. WaterGAP2 uses a runoff coefficient and two correction factors to calibrate the simulated and observed streamflow (Müller Schmied et al., 2014). Mac-PDM.20 is calibrated using the

generalized likelihood uncertainty estimation (GLUE) approach, comprising a 100,000-member ensemble based on different model parameterizations run with Watch Forcing Data and evaluated against Global Runoff Data Centre (GRDC) streamflow data (Smith, 2016). In mHM, calibration of global model parameters is performed against the daily observed streamflow of

275   GRDC stations, along with gridded global fields of FLUXNET evaporation (Jung et al., 2011) and a GRACE terrestrial water storage anomaly, using the ERA5 climate forcing (Landerer and Swenson, 2012). VIC uses the source datasets and parameter sets from Nijssen et al. (2001), namely the AVHRR-derived landcover dataset (Hansen et al., 2000) and the FAO soil textures (FAO, 1995), and is sub-sampled to $0.5° \times 0.5°$ via a nearest-neighbor approach. WAYS is calibrated against data from the International Satellite Land Surface Climatology Project (ISLSCP) Initiative II of the University of New Hampshire or GRDC

280   composite monthly runoff data (Fekete et al., 2011), from 1986 to 1995 at a $0.5°$ spatial resolution. These datasets are composite runoff data that combine simulated water balance model runoff estimates and monitored river streamflow (GRDC). CLM5.0 performs hydrological calibration in a Bayesian framework using a sequential Monte Carlo method (Lawrence et al., 2019). Five models (CLM4.5, DBH, MATSIRO, ORCHIDEE, and PCR-GLOBWB) adjust some parameters according to vegetation or soil properties, but they have no hydrologic calibration. Neither JULES-W1 nor LPJmL calibrate hydrology, although they

285   do calibrate biophysical processes and crop yield, respectively. MPI-HM and H08 are not hydrologic calibrated. Generally, GHMs are hydrologic calibrated based on their main goal of quantitatively simulating the continental water cycle.

4. Review of the global water models included in the study

Global water models were developed from the earliest land surface models created by Manabe (1969), Freeze and Harlan (1969), and Deardorff (1978). These first land surface models simulated the terrestrial water cycle by considering vegetation

290   processes, evaporation, soil moisture, and snow cover. Later on, Dooge (1982) identified the two major challenges of global hydrology: scaling and parameterization. Eagleson (1986) declared the necessity of global-scale hydrology. Inevitably, during the 1990s, the first global hydrological models were developed (Alcamo et al., 1997; Vörösmarty et al., 1998, Arnell, 1999). Over the years, many models have been developed and improved and many studies have been done to assess freshwater resources on the global scale (Bierkens, 2015).

295   In the present study, we analyze the state-of-the-art global water models included in the global water sector of the Inter-Sectoral Impact Model Intercomparison Project (ISIMIP: Frieler et al., 2017). GWMs simulate the terrestrial water cycle, on the global scale, and quantify water flows, water storage compartments, and human water use under past, current, and future climate and socioeconomic conditions. Some of these models also consider reservoir operations. In this study, GWMs do not simulate the ocean component of the global water cycle or water quality. They use input data at $0.5° \times 0.5°$ spatial resolution to obtain their

300   boundary conditions and parameters (Wada et al., 2017). Generally, these models are suitable for application over a minimum catchment size of 9,000 km^2 or at least four grid cells, at $0.5° \times 0.5°$ spatial resolution (Döll et al., 2003; Hunger and Döll, 2008). For smaller catchments, the results are often not reasonable (e.g., Beck et al., 2016) and require some corrections

305   Hattermann et al. (2017) highlighted the role of global and regional water models. Global water models assess the large-scale impacts of climate change and its variability, while regional water models assess the small-scale impacts that are specific to a particular river, catchment, or region. Gosling et al. (2017) underlined that the global and regional water models share many similarities regarding runoff simulation results and their conceptual approach to model development, although the GWM results vary more than regional water results.

310   Ultimately, GWMs have faced many challenges in selecting a good method to estimate water storage compartments, water flows, and human water use sectors. Some of these are presented in the following subsections.

4.1 Evaluation of global water ~~model~~ to observations

Many ISIMIP studies have evaluated the performance of GWMs for historical time intervals and have highlighted the importance of certain hydrological processes, in addition to many model shortcomings. For example, Wartenburger et al.

315   (2018) concluded that the values of actual land evapotranspiration are affected by the methods used to estimate evapotranspiration, number of soil layers, model structure, and uncertainties in the climate input datasets. Zaherpour et al. (2018) showed that GWMs overestimated mean and extreme monthly runoff, mostly because the ISIMIP precipitation dataset had too-high values and due to the method used to generate surface runoff. They recommended improving the prediction of low runoff and the magnitude and timing of seasonal cycles, investigating methods to calibrate models, testing models with

320   different parameter values, and examining the interconnected uncertainties (e.g., perturbed parameter ensembles: Gosling, 2013). Further, Veldkamp et al. (2018) identified that mean, high and low flows are improved by the parameterization of water abstractions and reservoir operations. However, these are also influenced by uncertainties regarding water abstraction sources, return flow sinks, and the timing of these issues. Masaki et al. (2017) reported that different simulated outflows from reservoirs depend on dam operation algorithms, with similar concepts in some cases, and on the simulated river inflows. Zhao et al.

325   (2017) highlighted the influence of the routing scheme on streamflow timing and magnitude and recommended inclusion of floodplain storage and backwater effects in models.

Scanlon et al. (2019) highlighted that GWMs underestimated GRACE-derived seasonal water storages amplitudes in tropical and (semi-)arid basins and overestimated them in northern high-latitude basins. They suggested to increase the number of soil layers in the models, improve the simulation of snow physics by including processes that delay snowmelt, improve

330   evapotranspiration schemes, and add surface water and groundwater storage compartments to some models.

GWMs were also evaluated a specific case: the 2003 European heatwave and drought (Schewe et al., 2019). The study showed that the models underestimated the streamflow on some European rivers, where no high anomalies were noticed, and underlined the need to further evaluate and improve the models for extreme conditions and to consider all optimistic and pessimistic results in an ensemble as hypotheses.

335   Nevertheless, GWMs must be evaluated for historical periods before making future projections, in order to validate their performance and reduce uncertainties (Krysanova et al., 2018; Do et al., 2020).

4.2 Climate impact assessments with global water models

Historical performance evaluation studies provide context for further work by evaluating modeled projections of climate change on irrigation water requirements (Wada et al. 2013) and the impact on regional and global water scarcity (Schewe et

340   al., 2014) and on hydrological drought (Prudhomme et al., 2014). The first two studies, Wada et al. 2013 and Schewe et al., 2014, explained the high variation of projected impacts of climate change on the irrigation sector and river discharge through the differences extant in the model structures. A fundamental conclusion of these studies was that hydrological model uncertainty is higher than climate model uncertainty. Prudhomme et al. (2014) underlined that models project little or even no increase in drought frequency if they include the active response of vegetation to CO_2 and to climate change in their structure.

345   Reinecke et al. (2020) highlighted less severe decreases of groundwater recharge, and even increases in some regions, when the CO_2 fertilization effect (*active vegetation*) is considered. Grillakis (2019) found that agricultural droughts (soil moisture droughts) are expected to increase in frequency. Milly and Dunne (2017) concluded that hydrological models overestimated potential evapotranspiration, causing overestimation of actual evapotranspiration and an underestimation of the runoff, in comparison with climate models.

350   Nevertheless, studies on water scarcity and their results are affected by their methodology, definitions, and assumptions.

4.3 Uncertainties of the global water models

Multi-model intercomparison studies showed a significant variation in the model results. One explanation could be that global hydrological modeling imposes uncertainties from forcing data, model parameters, processes included or excluded, and numerical algorithms used. Additionally, each modeling group has a different model development concept and purpose.

355   Ultimately, hydrology is an *inexact science* influenced by *aleatory* (random) and *epistemic* (lack of knowledge) uncertainties (Beven, 2018). Therefore, many models combined in an ensemble approach collect many uncertainties and structural differences.

It has been found that uncertainties of evapotranspiration and snow water equivalent depend on model structures and their algorithms, while uncertainties of runoff depend on climate forcing, specifically, precipitation (Haddeland et al., 2011;

360   Hagemann et al., 2013).

Other uncertainties derive from meteorological data (Müller Schmied et al., 2016); model structure complexity (Döll et al., 2016); parameter estimation (Samaniego et al., 2017); model calibration (Müller Schmied et al., 2014); future scenarios of greenhouse gas emissions, land use management, water management, and socio-economic patterns (Wada et al., 2016a). Finally, many studies concluded that the uncertainty of the hydrological results is primarily determined by the selection of

365   hydrological model and it exceeds the uncertainty caused by selection of climate model or emission scenario (Wada et al.,

2013; Schewe et al., 2014, Greve et al., 2018). Therefore, there is a need to better understand the models' structure complexity, their equations, and their approaches, and to improve the quality of the input data.

Some methodologies were also created on the catchment scale and they support the evaluation of multi-model structures and parameterizations, also considered as hypotheses on runoff generation, for example, analytical framework (Wagener et al.,
370 2001); the rejectionist framework (Vaché and McDonnell, 2006); Framework for Understanding Structural Errors (FUSE, Clark et al., 2008); SUPERFLEX (Fenicia et al., 2011); Catchment Modelling Framework (CMF, Kraft, 2012); Unifying Multiple Modelling Alternatives (SUMMA, Clark et al., 2015 a and b).

Other methodologies used in the evaluation of parameter values might be found in the Model Parameter Estimation Experiment (MOPEX: Duan et al., 2006), multiple-try DREAM(ZS) algorithm (Laloy and Vrugt, 2012), Generalized Likelihood
375 Uncertainty Estimation methodology (GLUE: Beven and Binley, 2014), perturbed parameter ensembles (Gosling, 2013), the Uncertainty Quantification Python Laboratory platform (UQ-PyL: Wang et al., 2016), Multiscale Parameter Regionalization (MPR, Samaniego et al., 2010 and 2017). Further, some studies have done multiple parameterizations of individual model compartments, to discover how these parameterizations influence the simulations: Essery et al., 2013 (testing 1701 snow models); Niu et al., 2011 (Noah-MP model); Pomeroy et al., 2007 (Cold Regions Hydrologic Model, CRHM); Kuppel et al.,
380 2018 (Ecohydrologic model, EcH2O). Therefore, these methods might offer some solutions for reducing the high number of parameters and their values still found in global water models, and to apply more reasonable regionalization schemes in global hydrological research (Bierkens, 2015).

Other methods can also be found in frameworks proposed by Döll and Romero-Lankao, 2017 and Kundzewicz et al., 2018.

In the end, Arheimer et al., 2020 showed that the catchment models can be applied at a global scale because of the new global
385 datasets, increased computational capacity, new methods to estimate parameters, and collaboration. Thus, GWMs may even become a part of the ESMs used to simulate the water cycle at a high resolution, including human water demand and use (Wood et al., 2011; Bierkens, 2015).

5 Similarities and differences among global water models

Similarities and differences among models are presented according to eight water stocks, five human water use sectors, and
390 desalination.

5.1 Similarities and differences in simulating water storage compartments

Canopy water storage. The changes in canopy water storage depend on how much water evaporates (canopy evaporation) and how much water is intercepted by canopy. Thirteen models include canopy water storage in their structure, while three other models do not include it (H08, Mac-PDM.20, and MPI-HM: Table S3). Ten models compute canopy water storage by
395 subtracting the throughfall amount and canopy evaporation from the total precipitation. Other three models (CLM4.5, CLM5.0, and MATSIRO) compute canopy water storage by subtracting the liquid or solid throughfall and canopy evaporation from the

precipitation intercepted by the canopy storage. MATSIRO is the only model that has two canopy water compartments: one for rainfall interception and one for snowfall interception. It also computes in detail how much water is intercepted by canopies in stormy areas with high wind speeds and in calm areas with low wind speeds. In these areas, precipitation depends, mainly,

400 on leaf area index (LAI) and water deficit in the canopy storage.

Three land surface models (CLM4.5, CLM5.0, and MATSIRO) divide total precipitation into precipitation intercepted by canopy, precipitation that penetrates the canopy and then reaches the ground (throughfall), and precipitation that falls directly on the ground (Tables S4–S6). Further, they also divide throughfall into liquid and solid phases.

Two models compute an interception scheme based on a leaf and stem area index, while seven models use only a leaf area

405 index (Tables 7 and 8). Ten models compute this considering vegetation type (a plant functional type system) (Tables 7 and 8). MPI-HM used prescribed data taken from Land Surface Parameter dataset version 2 (Hagemann, 2002). PCR-GLOBWB uses HYDE3.2 (Klein Goldewijk, 2017), MIRCA (Portmann et al., 2010), and GlobCover datasets (ESA GlobCover Project, 2005). Generally, prescribed vegetation ignores the decisive interaction between vegetation and runoff as well as interactions between the atmosphere and Earth's surface.

410 Throughfall is estimated by 13 models (Table S5) depending on 1. total precipitation and relative canopy water content (JULES-W1); 2. difference between total precipitation and canopy storage deficit (mHM, WaterGAP2, WAYS); 3. ratio between rainfall or snowfall and total precipitation (CLM4.5, CLM5.0, MATSIRO); 4. total precipitation and minimum value of potential evapotranspiration (PET) or canopy storage (LPJmL); 5. canopy water content (PCR-GLOBWB); 6. a function of LAI then weighted by the canopy fraction in the grid cell (DBH and ORCHIDEE); 7. canopy water content and grid cell

415 average precipitation (VIC); 8. total precipitation, canopy water content, and canopy evaporation (CWatM). Three models (H08, Mac-PDM.20, MPI-HM) do not estimate throughfall.

Four models (CLM4.5, CLM5.0, LPJmL, and ORCHIDEE; Tables 7 and 8) account for the CO_2 fertilization effect, in the LAI estimation, by using a photosynthesis scheme (*active vegetation* mentioned in section 2.1), and they have the ability to simulate the CO_2 effect on plant functioning. Generally, it was found that simulations depend on the number of PFTs prescribed or

420 defined in the model and on the processes used to estimate plants' ability to adapt, acclimate, and grow in new environmental conditions (Sitch et al., 2008).

Snow water storage accumulates snow below freezing and loses snow by melting and surface and/or snowdrift sublimation. GHMs use the degree-day method to compute snow accumulation and snowmelt, while LSMs use the energy balance method (Tables 7 and 8). Among GHMs, H08 is the only one that applies the energy balance method to compute snow accumulation

425 and melt. Additionally, three models (CLM4.5, CLM5.0, and CWatM) include glacier storage. CLM4.5 and CLM5.0 use a physically based snow module to calculate snow accumulation and melt; therefore, they include multiple snow layers where compaction, melt, refreezing, firn, and other snow related processes take place.

Four models (CLM4.5, CLM5.0, MPI-HM, and VIC) have two water storage compartments for snow: for estimation of frozen water and for liquid water content (Table S8). WaterGAP2 calculates snow accumulation and melting in 100 subgrid cells

430 using a degree-day algorithm (Schulze and Döll, 2004; Müller Schmied et al., 2014), while CWatM calculated using 3 to 10

elevation zones per grid. Five models (CLM5.0, DBH, JULES-W1, MATSIRO, and VIC) estimate snow held on the canopy, while ten models do not estimate it (Table S9). Further, seven models differentially estimate snow under the canopy (Table S10). Five models do not estimate sublimation: Mac-PDM.20, mHM, MPI-HM, PCR-GLOBWB, and WAYS (Table S11). MATSIRO is the only model that distinguishes between sublimation on snow-covered ground and snow-free ground. Snow

435   layers vary between 1 (most of the GHMs) and 12 (CLM5.0; Tables 7 and 8).

Soil water storage keeps and loses water from flows above and below the ground's surface. Hydrologically, this includes an unsaturated zone.

Soil hydrologic processes. Overall, 10 models consider initial infiltration as inflow of the soil storage, while 3 models (H08, JULES-W1 and WAYS) consider throughfall (Table S14). Mac-PDM.20 considers total precipitation as inflow of soil storage

440   (Table S14). All models compute surface runoff (Table S20), soil evaporation (Table S24), and infiltration (Table S25), while six models compute interflow (Table S26). Six models compute Hortonian overland flow (Table S21) and six models compute saturation excess overland flow (Table S22). H08 computes runoff properties varying according to the climate zone (Table 7). CLM4.5 includes an empirical soil evaporation resistance parameterization, while CLM5.0 includes a mechanistically based parameterization where the soil evaporation is controlled by a dry surface layer. Therefore, CLM5.0 has the ability to model

445   the seasonality of soil evaporation and soil water storage in (semi-)arid regions. It also explicitly simulates spatial variation in soil thickness (0.4 to 8.5 m) and columnar water holding capacity, unlike CLM4.5 (Lawrence et al., 2019). These models have a large number of soil layers, each having moisture storage potential depending on the soil texture. They use the same approach to calculate surface runoff and have the ability to compute liquid runoff and solid runoff from snow capping. Both models consider subsurface runoff as a product of an exponential function of the water table depth and a single coefficient (Niu et al.,

450   2005). VIC uses the variable infiltration curve (Zhao et al., 1980) to account for the spatial heterogeneity of runoff generation, and assumes that surface runoff from the upper two soil layers is generated by those areas where precipitation exceeds the storage capacity of the soil. The mHM model has one more bucket between the soil storage and groundwater storage named "unsaturated storage" representing the source for interflow and groundwater recharge.

LPJmL was adjusted, and the water from the uppermost soil layers is considered to contribute to surface runoff if excess of

455   storage is calculated according to the infiltration or percolation rates, which depend on soil type. LPJmL routes, what was previously lateral runoff, from "layer 0" (first 20 cm), as surface runoff.

In JULES-W1, water that reaches the soil surface is split between water that infiltrates into the soil and surface runoff. Infiltration takes place at a rate equal to saturated hydraulic conductivity multiplied by an infiltration enhancement factor, which is dependent on the presence and type of vegetation. If a soil layer becomes saturated, the water in excess of saturation

460   is put into the layer below. JULES-W1 also uses a "zero-layer" scheme that does not use explicit model layers to represent snow, instead adapting the topsoil level to represent lying snow processes (Best et al., 2011). WAYS simulates the water storage and flows in soil only for the entire root zone (Table 8). In the DBH model, runoff is generated directly when soil layer is saturated, or is generated when rainfall intensity is larger than the infiltration rate estimated with the Green–Ampt method (Tang et al., 2006).

465   Two models (CWatM and MPI-HM) have an additional water storage compartment to compute the runoff concentration in a
       grid cell that has a lag time before entering the river storage compartment (Table S19). Consequently, this storage serves to
       create a delay between runoff and streamflow, and accounts for the average distance that runoff, generated at a specific point
       within a grid cell, has to travel before reaching the river. This storage collects water from rivulets and creeks or concentrates
       runoff in rivulets and creeks before it enters the river storage, because the rivulets and creeks are smaller than the size of a

470   single grid cell and have different water retention properties from the main river channel within the grid cell. Therefore, this
       compartment does not act as a floodplain, to delay floods, or as overland flow, to express too much water in the soil. In its
       original structure, MPI-HM named this compartment "overland flow", but we decided to rename it "rivulet storage" to avoid
       confusion among readers.

       Some GWMs compute vertical water movement in unsaturated soils by applying the Richards equation (Richards, 1931; e.g.,

475   CLM4.5, CLM5.0, CWatM, JULES-W1, MATSIRO, ORCHIDEE, VIC). However, the Richards equation might be not
       relevant for the models that have one soil layer. LPJmL uses a percolation scheme to estimate vertical water movement that
       applies the storage routine technique developed by Arnold et al. (1990) and simulates free water in the soil bucket. DBH uses
       the Green–Ampt equation to compute infiltration in unsaturated soils.

       Two models (CWatM, LPJmL) compute percolation (infiltration below the root zone; Table S27). Five models compute

480   capillary rise (CLM4.5, CLM5.0, CWatM, MATSIRO, and PCR-GLOBWB), with CWatM and PCR-GLOBWB using the
       same approach (Table S28).

       Soil column configuration. Number of soil layers ranges between 1 (H08, MPI-HM, and WaterGAP2) and 25 (20 soil layers
       + 5 bedrock layers: CLM5.0), while total soil depth is between 1 m (H08) and 49.6 m (CLM5.0; Tables 7 and 8). ORCHIDEE
       uses a relatively deeper soil column to account for soil thermic. LPJmL has five hydrologically and thermal active soil layers

485   plus one thermal active soil layer. MPI-HM defines soil storage in terms of the maximum water column, varying between 0
       and 5 m; therefore this cannot be translated into soil depth directly. Five models (CLM4.5, CLM5.0, CWatM, MATSIRO, and
       VIC) compute frozen soil (Table S13).

       Groundwater storage, beneath the soil water storage compartment, receives water from seepage and groundwater recharge.
       It loses water through capillary rise, groundwater runoff, and abstraction for human water use. Hydrologically, it includes the

490   saturated zone or phreatic zone. Eleven models include groundwater storage in their structure, and most of them have only one
       groundwater layer (Tables 9, 10, S29). In ISIMIP2b, two models (JULES-W1 and LPJmL) consider the water excess from the
       bottom soil layer as *seepage* and relate this variable with *groundwater runoff* and *groundwater recharge* because they do not
       have a groundwater compartment.

       CLM4.5 simulates an unconfined aquifer parameterization as a groundwater component, below the saturated soil storage and

495   with a prescribed maximum value (5000 mm), while CLM5.0 simulates an impermeable bedrock with five layers and therefore
       assumes no groundwater flow as bottom boundary conditions. In CLM4.5, the unconfined aquifer interacts with the saturated
       soil storage through the water table, whether it is within or below this storage. When the water table is below the soil storage,
       the aquifer recharge is estimated by applying Darcy's law across the water table (Lawrence et al., 2019).

MATSIRO has a dynamic groundwater scheme (Koirala et al., 2014; Pokhrel et al., 2015) in which the number of soil layers
500   in the saturated zone (i.e., groundwater) varies in time depending on water table location between 1 and 13 (Table 7). The two-
way interaction between the unsaturated zone (for which vertical moisture movement is resolved by solving the Richards
equation) and the underlying aquifer is simulated through moisture flux exchange at the water table. This flux exchange is
determined as the algebraic sum of downward gravity drainage from the unsaturated soil layer overlying the water table and
the upward capillary flux (Koirala et al., 2014; Pokhrel et al., 2015). The water balance of the saturated zone is resolved by
505   considering recharge to the groundwater aquifer and groundwater runoff that is determined by using a two-parameter,
statistical-dynamical formulation considering soil hydraulic properties and basin geomorphology (Yeh and Eltahir, 2005). The
variation in the water table is also determined by the aquifer specific yield.

In Mac-PDM.20, it is assumed that all water in excess of field capacity drains in one day to the deep store, which for ISIMIP2b
is used to represent groundwater recharge (R_{gwr}). The total runoff (q_{tot}) is the sum of direct runoff (q_s) plus delayed runoff from
510   the deep soil and groundwater (q_{sb}). This delayed runoff (q_{sb}) is assumed to be a non-linear function of the amount of water
held in the groundwater and deep soil store (Table S31). Thus, like with MPI-HM, the purpose of the delayed runoff (or
baseflow) is predominantly to cause a delay in river discharge and not to simulate groundwater in detail.

H08 separates groundwater into renewable and one nonrenewable layers (Hanasaki et al., 2008). WaterGAP2 is the only model
that simulates the groundwater recharge from surface water bodies in semiarid and arid grid cells (Döll et al., 2014).
515   Fourteen models compute groundwater recharge, three using the same approach (H08, WaterGAP2, and WAYS: Döll and
Fiedler, 2008; Table S30), while twelve models compute groundwater runoff (Table S31).

Lake storage fills with water through flows above and below the ground and stores water for a certain residence time. It loses
water through discharge to other storages, evaporation, groundwater recharge, and water abstraction for human water use. Ten
models do not include lakes (Tables 9 and 10). Five models compute evaporation from lakes, three of them based on a PET
520   approach (Table S33), while four models compute outflow from lakes (Table S34). CLM4.5 and CLM5.0 compute the lake
storage as virtual storage where the difference between precipitation and evaporation is balanced automatically by their
outflow, named *lake runoff*. CLM4.5 uses constant lake depth, while CLM5.0 uses spatially variable lake depth, and freezing
and thawing are included in the lake body (Vanderkelen et al., 2020).

LPJmL treats natural lakes and rivers in a similar way in terms of inputs and output. Lake inputs to a river can also include
525   upstream river inputs to the lake. LPJmL also keeps track of a lake fraction in the river input. WaterGAP2 and CWatM have
two types of lake storage: "local lake storage", gets water from runoff resulting within the cell, and "global lake storage", gets
water from runoff resulting within the cell and the upstream cell (Döll et al., 2012). For ISIMIP2b, MPI-HM has used the
prescribed wetlands and lakes extent, taken from the Land Surface Parameter dataset 2 (Hagemann, 2002).

Reservoir storage fills with water behind dams through flows above and below the ground and stores water for a residence
530   time. It loses water through discharge to other storages, evaporation, groundwater recharge, and water abstraction for human
water use. Ten models (CLM4.5, CLM5.0, DBH, JULES-W1, Mac-PDM.20, mHM, MPI-HM, ORCHIDEE, VIC, and
WAYS) do not include reservoir storage for ISIMIP2b (Tables 9, 10, S35). Further, only WaterGAP2 simulates explicitly the

reservoirs, lakes, and wetlands (Tables 9 and 10). Six models compute outflow from reservoirs (Table S37), while evaporation from reservoirs is computed by four models (Table S38).

535 In general, most of the models use the Global Reservoir and Dam database (GRanD: Lehner et al., 2011), but with a different number of active managed reservoirs, used for reservoir operation during simulations. Three models (LPJmL, WaterGAP2 and PCR-GLOBWB) merge more than one reservoir per grid cell into one reservoir, if required.

Four models (CWatM, H08, MATSIRO, and WaterGAP2) use two water compartments, global and local reservoirs, to represent the reservoirs, following the reservoir algorithm developed by H08. However, there are some differences on how the 540 scheme was implemented in the models, mainly, because of model structure, but the approach is essentially the same. These four models use the same approach in selecting active managed reservoirs for reservoir operation, but they use different thresholds. WaterGAP2 considers 1109 active managed reservoirs and handles reservoirs below 0.5 km^3 storage capacity as local lakes. MATSIRO considers only 728 out of 6862 reservoirs for reservoir operation. In MATSIRO, global reservoirs have more than 1 km^3 total storage capacity and "local reservoirs" or "ponds" have less than 1 km^3 (around 6134 reservoirs; Hanasaki 545 et al., 2006; Pokhrel et al., 2012a and b). H08 considers 963 active managed reservoirs (global reservoirs) and 5824 local reservoirs; therefore, global reservoirs regulate river flow, while local reservoirs do not. Global reservoirs have 4773 km^3 of total storage capacity, while local reservoirs have 1300 km^3 of total storage capacity. In H08, when multiple local reservoirs are present in a grid cell, their capacity is added together. CWatM considers 3663 active managed reservoirs, while PCR-GLOBWB considers 6177. LPJmL includes 4134 reservoirs that become active after the first year of operation. In LPJmL, 550 reservoirs are not managed according to an operation scheme, they are modeled as lakes with a maximum storage amount and the water over this amount is released as reservoir outflow; irrigation water can also be taken from the reservoir.

Five models (CWatM, H08, LPJmL, MATSIRO, and WaterGAP2) use a retrospective reservoir algorithm, while one model (PCR-GLOBWB) uses a prospective reservoir algorithm. The retrospective reservoir algorithm uses river flows and water demand, which were processed in a previous step, while the prospective reservoir algorithm uses predicted river flows and 555 water demand (van Beek et al., 2011).

Wetlands storage fills and empties with water similarly to lake and reservoir compartments. Two models (MPI-HM and WaterGAP2) compute wetland compartment, evaporation, and outflow from land (Tables S39–S42). WaterGAP2 has two types of wetland storage: "local wetland storage", which obtains water from runoff resulting within the cell, and "global wetland storage", which obtains water from runoff resulting within the cell and the upstream cell (Döll et al., 2012).

560 **River storage** fills with water through flows above and below the ground. It loses water through streamflow, evaporation, channel transmission, and water abstraction for human water use. Five models (DBH, JULES-W1, Mac-PDM2.0, VIC, WAYS) do not include river storage for ISIMIP2b simulations, because of computational and resource constraints, nor do they compute streamflow (Tables 9, 10, S43, and S46). Four models (LPJmL, MATSIRO, MPI-HM, WaterGAP2) use a linear reservoir cascade approach to compute the water balance of the river storage (Tables 9 and 10). Furthermore, MATSIRO uses 565 Total Runoff Integrating Pathways (TRIP) for river routing through a channel. Three models (CWatM, H08, and LPJmL) consider the minimum release for environmental flow. CWatM adopts a kinematic wave approach, approximation of the Saint-

Venant equation (Chow et al., 1998), linked with dynamic reservoir and lake operation. Further, CWatM computes runoff concentrated in creeks and rivulets, with a lag time before entering the river storage, by using a triangular weighting function (Burek et al., 2020). ORCHIDEE includes a river transport module that involves the Simulated Topological Network (STN-30p). PCR-GLOBWB uses a travel time routing (characteristic distance) linked with dynamic reservoir operation. For runoff and streamflow simulation, CLM4.5 uses a river transport model (RTM), while CLM5.0 uses a new physically based runoff routing model, called the Model for Scale Adaptive River Transport (MOSART; Oleson et al., 2013, Lawrence et al., 2019). The mHM model uses a mesoscale routing model with an adaptive time step according with the spatially varying celerity (Thober et al., 2019). Only MPI-HM and ORCHIDEE include a routing model with a wetlands and floodplain scheme, in which wetlands act as floodplains. Furthermore, ORCHIDEE includes swamps.

Six models (CLM5.0, CWatM, MPI-HM, ORCHIDEE, PCR-GLOBWB, WaterGAP2) apply the Manning–Strickler equation to estimate river flow velocity and use various values for it. CLM4.5 uses a standard river flow velocity of 0.35 m s^{-1}, while H08 and MATSIRO use 0.5 m s^{-1} (Tables 9 and 10). LPJmL considers a standard river flow velocity of 1 m s^{-1}. MPI-HM uses the Manning–Strickler equation only for flow velocity computation in wetlands, while, for rivers, it computes a slope-dependent flow velocity following the approach by Sausen et al. (1994).

Inflow from upstream grid cell surface water bodies represents the sum of inflow water from neighboring upstream grid cells for CLM4.5, CLM5.0, CWatM, mHM, and WaterGAP2 (Table S45). Additionally, CWatM and WaterGAP2 route this water also through lakes and reservoirs before it reaches its final point. H08 computes it as being the product between a 0.5 m s^{-1} flow velocity and river storage from upstream grid cells. LPJmL considers it as being the outflow of river storage reduced by evaporation from lakes and reservoirs, while MPI-HM considers it as being the sum of outflow from rivulet storage, groundwater runoff, and streamflow from the upstream grid cells, then reduced by inflow from the wetland of an upstream grid cell. MATSIRO considers it as being the sum of inflow water from the neighboring upstream grid cell multiplied by outflow of river from an upstream grid cell. ORCHIDEE calculates it as being the sum of stream river storage of upstream grid cells divided by topographic index of the retention time and a reduction factor of stream river storage. PCR-GLOBWB takes into account the outflow from river storage, time of process duration, length of river sections, and the coefficient friction of the reservoir weir.

Evaporation from rivers is computed only by three models, CWatM, LPJmL, and PCR-GLOBWB, based on a PET approach (Table S47).

5.2 Similarities and differences in simulating human water use sectors

Some GWMs simulate water extracted from surface water compartments and/or a groundwater compartment that is used for human activities. Human water abstraction represents the sum of the water consumed by humans, evaporative and speculative water losses (named *water consumption*), and water returned to the groundwater or surface water compartments (named *return flow*, being the part of the water not consumed). Generally, three models extract water for human activities from groundwater

or surface water bodies (H08, PCR-GLOBWB, and WaterGAP2). Seven models (DBH, JULES-W1, Mac-PDM.20, mHM,
600 ORCHIDEE, VIC, and WAYS) do not include any human water use sectors in their structures (Table 6).

Irrigation sector. Irrigation water demand (potential irrigation water abstraction) is computed by three models (Table S52).
Groundwater abstraction and its consumption for the irrigation sector is simulated by five models (CWatM, H08, MATSIRO,
MPI-HM, and WaterGAP2: Tables S53 and S54), while three models explicitly compute the return flow (Table S55). Irrigation
surface water abstraction is calculated by nine models (Table S56, Tables S100–S101). CWatM includes a "normal irrigation
605 scheme", to mimic rainfall when the plants need it, and a paddy rice irrigation scheme, to mimic the flooding of the rice area
(Table S56).

The main water source for the irrigation sector is *river* for nine models (CLM4.5, CLM5.0, CWatM, H08, LPJmL, MATSIRO,
MPI-HM, PCR-GLOBWB, WaterGAP2), and then the secondary source is *groundwater* for six models (CWatM, H08,
MATSIRO, MPI-HM, PCR-GLOBWB, WaterGAP2). Five models take water from lakes for the irrigation sector and four
610 models take water from reservoirs. Only two models take water for irrigation from the ocean (Figure 1). Return flows from
irrigation sector recharge the soil (seven models), groundwater (seven models), and rivers (six models), while the return flows
from domestic and manufacturing recharge lakes (three models), reservoirs (two models), and rivers (five models; Figure 2).

Domestic, livestock, and industry sectors. Generally, four models (H08, MATSIRO, PCR-GLOBWB, and WaterGAP2)
simulate water abstraction, water consumption, and return flow for the domestic (household: Tables S59–S64) and
615 manufacturing sectors (Tables S69–S74). MATSIRO and LPJmL used prescribed data for water demand of the domestic and
industry sectors, offered by the ISIMIP2b framework, representing annual sums divided evenly over all days. These input
datasets provide water consumption, but not return flow from these sectors. Consumption water can return to the atmosphere
as evapotranspiration. LPJmL used prescribed data for domestic and industrial water consumption data and assumed that only
the consumed water amount is withdrawn. MATSIRO used prescribed data for domestic and industrial water demand and it
620 computed itself the water abstraction and consumption for these sectors, by applying a simple approach. ISIMIP2b does not
offer prescribed data for livestock sector. MATSIRO combines manufacturing and electricity sectors in one sector, the industry
sector. PCR-GLOBWB computes amount of water abstracted and consumed for livestock sector, taken from groundwater and
surface water bodies (Tables S65–S68), while WaterGAP2 computes only the amount of water taken from surface water bodies
(Tables S67–S68). WaterGAP2 is the only model that computes amount of water abstracted and consumed for electricity sector
625 (Tables S75–S76).

Total groundwater abstraction (Table S77) is computed differently by MATSIRO, MPI-HM, and WaterGAP2. MATSIRO
and WaterGAP2 take similar approaches: groundwater abstraction for the irrigation sector is reduced by the sum of
groundwater abstraction for the domestic and industry sectors. MPI-HM considers the total as being equal only to groundwater
abstraction for the irrigation sector, as other sectors are not included in the model.

630 **Total lake abstraction** (Table S78) is computed differently by LPJmL, MPI-HM, PCR-GLOBWB, and WaterGAP2. LPJmL
sums the gross irrigation requirement and household, industry, and livestock demand in the grid cell, with gross irrigation
requirement and household, industry, and livestock demand in the downstream grid cell. MPI-HM considers lake abstraction

equal to surface water abstraction for the irrigation sector, while PCR-GLOBWB sums water abstraction demand for the industry, irrigation, domestic (household), and livestock sectors. WaterGAP2 computes it as the sum of water abstraction for

635 the irrigation, livestock, domestic, manufacturing, and electricity sectors taken from surface water bodies. The net surface water abstraction is satisfied in WaterGAP2 in the following order: 1) river, 2) global lakes and reservoirs, and 3) local lakes.

Total reservoir abstraction (Table S79) is computed differently by H08, LPJmL, MATSIRO, PCR-GLOBWB, and WaterGAP2. H08 considers it as being sum of monthly water abstraction for the irrigation, industry, and domestic sectors. LPJmL adds up the gross irrigation requirement and household, industry, and livestock demand at the grid cell with the gross

640 irrigation requirement and household, industry, and livestock demand at the downstream grid cell (similar to lake abstraction). MATSIRO adds up water abstraction from reservoir for the domestic, industry, and irrigation sectors, while PCR-GLOBWB adds water abstraction demand for the industry, irrigation, domestic (household), and livestock sectors (similar to lake abstraction). WaterGAP2 sums up water abstraction for the irrigation, livestock, domestic, manufacturing, and electricity sectors taken from surface water bodies. The net surface water abstraction is satisfied in WaterGAP2 in the following order:

645 1) rivers, 2) global lakes and reservoirs and 3) local lakes.

Total river abstraction (Table S80) is computed by CLM5.0 and WaterGAP2. WaterGAP2 considers it as the sum of water abstraction for the irrigation, livestock, domestic, manufacturing, and electricity sectors taken from surface water bodies. The net surface water abstraction is satisfied in WaterGAP2 in the following order: 1) rivers, 2) global lakes and reservoirs and 3) local lakes (similar to lake and reservoir is equal to surface water bodies).

5.3 Similarities and differences in simulating desalination

Seawater abstraction, consumption, and return flows (Tables S81–S83) are computed only by H08 (Hanasaki et al., 2018). Seawater abstraction represents the sum of seawater abstraction for the municipal and industry sectors. Three conditions must be met in order to use desalination: i) GDP > USD 14,000 person year^{-1} in terms of purchasing power parity (PPP); ii) humidity index below 8%; iii) within three grid cells of the seashore. It is assumed that seawater desalination is not used for irrigation

655 and that all demand for municipal and industrial water is abstracted by desalination if available. In the context that desalination is not used for irrigation, seawater consumption represents seawater abstraction weighted by the ratio of consumption to withdrawal, which is equal to 0.1 and 0.15 for industrial and municipal water use. Return flow from seawater abstraction represents seawater abstraction weighted by the non-used fraction (0.1 and 0.15 for industrial and municipal water use) and proportion lost during delivery (set to zero).

5.4 Examples of how parameterization can differ between GWMs

Different equations used by GWMs led to different model results, for example, different evapotranspiration methods led to significant differences in runoff estimation (Gosling and Arnell, 2011b; Kingston et al., 2009). The equations include parameters that are used to calibrate GWMs. The application of different parameter values can lead to different results between

models (as can the employment of different model structures). For example, we present how global water models simulate the
groundwater recharge and the maximum value of canopy storage differently.

Groundwater recharge (Table S30) is computed by 14 models. JULES-W1 and LPJmL do not include in their structure
groundwater storage and seepage (the water that seeps from the last soil layer), which was reported as groundwater recharge
and groundwater runoff for ISIMIP2b. CLM4.5 and CLM5.0 use the same approach to compute groundwater recharge, by
using the concept of soil matrix potential and considering the hydraulic conductivity of the layer containing the water table.
CWatM and PCR-GLOBWB use the same approach by reducing percolation with capillary rise, but CWatM also considers
preferential flow as inflow. DBH estimates it depending on potential soil water content multiplied by the soil depth layer and
maximized by soil hydraulic conductivity. Three models (H08, WaterGAP2, and WAYS) consider it as being the minimum
value between maximum groundwater recharge and total runoff from land, weighted by a relief-related factor, a soil texture-
related factor, a hydrogeology-related factor, and a permafrost- and/or glacier-related factor (Döll and Fiedler, 2008). Further,
WaterGAP2 sets (semi-)arid grid cells, sandy texture, and grid cells with throughfall equal or below 12.5 (mm day^{-1}) to 0.
MATSIRO estimated groundwater recharge as being the variation of unfrozen soil moisture over time. MPI-HM equals
groundwater recharge to percolation. ORCHIDEE estimates it depending on relative soil water content, but it is capped down
to 0 and maximized by groundwater runoff.

Maximum value of canopy storage (Table S7). Another example is that the models estimate differently the maximum value
of canopy storage and leaf area index (LAI) values. WaterGAP2 and WAYS estimate the maximum value of canopy storage
by multiplying 0.3 mm with LAI. Further, WAYS estimates seasonal LAI depending on the growing-season index, day length,
and the actual root zone water storage. The root zone soil moisture stress parameter is fixed at 0.07, while WaterGAP2
estimates LAI based on a simple growth model and based on land cover characteristics (Table S7). VIC multiplies 0.2 mm by
the monthly LAI. Additional, VIC takes into account aerodynamic and architectural resistances. CWatM equals maximum
value of canopy storage with LAI that varies every 10 days depending on land use classes.

5.5 How many water flows, water storage compartments, and human water use sectors are included in the GWMs?

One way of showing the number of equations and/or parameterization schemes that comprise a model is to count the number
of water flows, storage compartments, and use sectors existent in each model participating in ISIMIP2b. Generally, GHMs
have a high number of water storage compartments because their main purpose is to simulate the water cycle. LSMs and
DGVMs have a relatively smaller number of process (in this count), but each process is simulated in a more sophisticated way
or has a physically based representation. LSMs exclude some hydrological processes because they are not relevant for their
research purpose, spatial resolution, or cannot be parametrized in a general manner, adding some uncertainty.

In this study, WaterGAP2 includes the highest number of water storage compartments (11; see Figure 3), while JULES-W1,
Mac-PDM.20, and VIC have the lowest, three water compartments (Figure 3). Others include CWatM, with ten compartments,
then MATSIRO (seven compartments), followed by seven models (CLM4.5, CLM5.0, H08, LPJmL, mHM, MPI-HM, and
PCR-GLOBWB) with six compartments. Seven models do not simulate water used by humans for economic purposes such as

irrigation, domestic, livestock, manufacturing, electricity, and desalination (Figure 4). Four models (CWatM, MATSIRO, H08, and LPJmL) combine the manufacturing and electricity sectors in one sector: the industry sector. WaterGAP2 simulates five human water use sectors. Three models (H08, PCR-GLOBWB, and CWatM) simulate four human water use sectors and one

700 model (MATSIRO) simulates three. Four models (CLM4.5, CLM5.0, LPJmL, and MPI-HM) simulate only water used by humans for the irrigation sector. WaterGAP2 has the highest number of water flows (22) to simulate water use, while MPI-HM has the lowest number (2; Figure 4).

6 Challenges and potential in global hydrological modeling

6.1 Challenges in making this intercomparison study

705 We encountered many challenges in harmonizing terminology among the 16 global water models, as well as among climate, global hydrological, and vegetation communities. It was challenging to intercompare the global water models using their different style in describing the model structure, defining the variables, and writing the model equations. Therefore, we decided to create a standard writing style for model equations, presented in subsection 3.2, and to decide upon clear definitions of the analyzed variables.

710 We discovered that, in some models, *groundwater runoff* and *baseflow* are used synonymously and define the water that leaves groundwater storage. We also found that *baseflow* and *subsurface runoff* are used synonymously, and define the amount of water estimated for the third soil layer (VIC). Hence, we decided to use *subsurface runoff* synonymously with *interflow* and to define it as the amount of water that leaves the soil layer laterally. In this paper, *baseflow* is considered to be the low part of the streamflow that is supplied by groundwater, drainage from lakes, wetlands, glaciers, and interflow during long periods

715 when no precipitation or snowmelt occurs. Ultimately, we have excluded the variable *baseflow* from the analysis because it is not simulated by GWMs in ISIMIP2b.

MPI-HM includes additional storage, called *baseflow storage*, that collects the drainage leaving through the bottom of the soil storage and applies a substantial time lag before passing it on to the river storage. In ISIMIP2b, the drainage computed by MPI-HM was submitted as subsurface runoff, but considering that this baseflow storage acts similarly to a groundwater

720 storage, drainage could be used as groundwater recharge in ISIMIP3a/b. Consequently, its outflow could be submitted as groundwater runoff. However, the purpose of this baseflow storage is predominantly to cause a delay in river discharge and not to simulate groundwater in detail.

We also found out that the words *drainage* (MPI-HM)*, aquifer recharge* (CLM4.5)*, and *groundwater recharge* (GHMs) are used synonymously to define the amount of water that reaches the groundwater storage. In this case, we decided to use only

725 *groundwater recharge*, because of its hydrological meaning.

We define *percolation* as the amount of water that infiltrates beyond the root zone and *seepage* as the amount of water that leaks at the bottom of the soil storage. We relate *seepage* with *groundwater recharge* and *groundwater runoff* for the models that do not include a groundwater storage, supposing that this water would reach groundwater storage if it would exist.

Another discovery was that *throughfall* and *drip* in some models were considered synonyms and they were used to describe
730   precipitation that falls to the ground through canopy spaces (CLM4.5, CLM5.0, MATSIRO). In this case, we decided to
separate these words and to define *throughfall* as being precipitation that falls to the ground through canopy spaces and *drip*
as being precipitation that leaks at the edge of canopy.

We conclude that within hydrology and among communities there is great confusion regarding the terminology used, including
the variables and their definitions. Therefore, we need to communicate, interact, and engage to clarify the meaning of the
735   words and processes, and to facilitate easier communication, understanding, and analysis.

6.2 Challenges in global hydrological modeling

Simulating the terrestrial water cycle on the global scale involves many challenges. These various challenges were identified
by reviewing articles published by the climate, global hydrological, and vegetation communities (Table 11). The challenges
have been classified according to the 23 unsolved problems in hydrology (UPH), identified by Blöschl et al., 2019, to
740   harmonize the efforts of the global and catchment hydrological communities. These challenges can generally be overcome
through the development of new datasets, innovative and creative collaboration among communities, and investment in
technical infrastructure.

6.3 Recommendations for multi-model intercomparison projects

Multi-model intercomparison projects (MIPs) are based on communication and collaboration. Ideally, through collaboration,
745   communities will fill in existing knowledge gaps, improve the quality of the input data and the processes in the models, and
implement the missing processes in the models.

Wagener et al., 2020 well described the hydrological knowledge gaps as *hydrologic lions*, similar to the knowledge gaps of
medieval maps represented as lions. They proposed focusing hydrological research on openly shared perceptual models,
inclusion of metadata for each hydrologic study (e.g., location and time period covered by a study), and effective knowledge
750   accumulation. In addition to these statements, we also propose focusing on effective collaboration that starts with effective
wish lists, including specific research questions, goals to answer these questions, methods to achieve the goals, datasets to be
used, and tasks to be done.

We encourage communities to write and convey clear, simple, and understandable texts for large audiences. We consider that
simplicity improves communication, and communication starts with a common language, the same words having the same
755   meaning for the sender and the receiver. Theoretically this is possible, but in practice, there are some discrepancies among
scientists (highlighted in subsection 2.2), as well as between scientists and stakeholders, as revealed by Sultan et al. (2020).
They underlined that scientists and stakeholders use vocabulary differently in climate impact science.

The review of GWMs, presented in section 4, highlights the need to design hydrological inter-model comparison studies by
nominating models or research questions according to some specific criteria, for example, (i) specific model compartments
760   (Nazemi & Wheater, 2015; Wada et al., 2017), (ii) specific evaluation metrics (Gupta et al., 2009; Veldkamp et al., 2018;

Zaherpour et al., 2018), (iii) locations of specific hydrological indicators, regions, or rivers (Masaki et al., 2017; Veldkamp et al., 2018). These studies still emphasized the need to improve the quality of the input data, upgrade the hydrological processes in the models' structure, integrate missing hydrological processes, and further reduce uncertainties.

We recommend, for the benefit of the multi-model intercomparison projects, to 1. maintain very good documentation of the model code; 2. always start research with a list, for example, with water storage compartments, flows, and human water use sectors included in the model structures; 3. have clear definitions of the variables, water storage compartments, flows, and human use sectors, describing exactly their role in the model; 4. have synonyms for variables, helping to show similarities and differences among models; 5. collect all ideas, recommendations, and improvements received from everyone (in our case, they were required to complete our study); 6. collaborate and communicate with peers, which was very useful in our study for identifying synonyms among communities; 7. describe *your model* or *a model* through *your eyes* and *other's people eyes*; 8. invest much time and patience and be meticulous about extracting equations of water storage, flow, and human water use sectors from the model code.

Our future research will include describing the GWMs analyzed in this study, through a standard visualization of the water cycle that will show the water storage compartments, water flows, and human water use sectors included in the ISIMIP2b model structures. These diagrams would be connected with the tables presented in the supplement of the present paper (Tables S1–S83).

We affirm that model intercomparison projects need to organize workshops on model parameterization including some *parameterization* experiments and some evaluation studies on the equations applied to compute water storage compartments, water flows, and human water use sectors, as well as considering model outputs. We also note that this review and description study had a positive impact on the modeling groups, motivating them to re-think and re-analyze model structures, equations, and descriptions.

6.4 Potential future research in global hydrological modeling

In this study, we analyzed the GWMs version used for ISIMIP2b. Hence, in their original structure, these models include some water stocks, water flows, and human water use sectors that have not been used for ISIMIP2b. In this section, we present potential future research for the 16 analyzed modeling groups (Tables S102 and S103).

Some GWMs, such as gridded models, have the ability to operate at various spatial–temporal scales: CWatM, CLM4.5, CLM5.0 (3 h time step at around 11 km).

Numerous developments are ongoing within the CLM team and can be followed on the model's GitHub page (https://github.com/ESCOMP/CTSM). Active developments include the improvement of the irrigation scheme (Thiery et al., 2017; 2020), the representation of land cover and land management (Meier et al., 2018; Hirsch et al., 2017; 2018), and the implementation of reservoirs (Hauser et al., 2019).

CWatM developed, in addition ISIMIP2b, a groundwater scheme with linkages to MODFLOW for 5 arcmin and 30 arcsec spatial resolution. The CWatM modeling group plans to develop a reservoir storage including different operation schemes

(e.g., energy, irrigation), to increase the temporal resolution (at 1 h), to apply a global calibration also for ungauged catchments,

795 such as using the Budyko framework (Greve et al. 2020), applying both the day-degree method and energy balance method to estimate snow accumulation and melt, and applying several methods to estimate evaporation based on changing CO_2 concentration.

DBH plans to include human water uses (industrial and domestic sectors), either by developing a new module or using the simulations from other models (e.g., WFaS dataset), to calibrate the model in the new ISIMIP3 simulation round, and to

800 improve the input/output module to read and write netcdf files.

The H08 modeling team used an approximate Bayesian computation technique to calibrate four parameters that are transferred to other regions containing no observations, mainly, based on Köppen–Geiger regions. The modeling group also increased the spatial resolution to 5 min and improved the representation of crops used for biofuel in the model.

The JULES-W1 modeling group plans to make a technical update that will enable the river routing module to estimate

805 discharge.

The LPJmL group developed an improved energy balance module and soil hydrological scheme that can estimate permafrost dynamics (Schaphoff et al., 2013) and made the model source code freely available on GitHub (https://github.com/PIK-LPJmL/LPJmL; Schaphoff et al., 2018), hoping to engage a broader scientific community in LPJmL model development and applications.

810 The Mac-PDM.20 modeling group plans to develop a water use module.

MATSIRO modeling group has implemented a land-use change process, terrestrial biogeochemical processes, and an additional crop growth process into MATSIRO to develop a new modeling framework. As key interactions are taken into account and all processes are coupled, important boundary conditions for hydrological simulations can be dynamically simulated internally. This hydrological simulation modeling framework has been coupled with MIROC GCM and has been

815 used as an Earth system model. In addition, the group recently proposed new schemes for lateral groundwater flow, water temperature, and sediment transportation.

Ongoing efforts to improve the realism of hydrologic processes in the mHM include the development of the multiscale lake module (mLM), a comprehensible framework for reservoir regulation as well as natural processes in lakes. Near-future developments will focus on a glacial module, to better account for processes in cold regions, as well as coupling it to a

820 groundwater model that will replace the current linear groundwater reservoir.

The MPI-HM modeling group plans to increase the spatial resolution of regional versions. The group currently implemented canopy storage in the latest model version and is developing experiments to integrate reservoir storage.

The ORCHIDEE group is focusing on calibration, soil storage, groundwater storage, river storage, reservoir storage and wetland storage (MacBean et al., 2019; Verbeke et al., 2019; Yin et al., 2020; Schrapffer et al., 2020; Mizuochi et al., 2020).

825 The PCR-GLOBWB modeling group plans to increase the temporal and spatial resolution of the input data, to increase the temporal resolution (3 h) for energy balance calculations and the global spatial resolution (1 km), to improve the soil

representation by including the Richards equation, to add more snow elevation layers, to include additional fast runoff component for improving daily discharge simulations, and to improve the reservoir operating scheme (Sutanudjaja et al., 2018). The VIC modeling group developed different irrigation practices (Shah et al., 2019a and b) and included a reservoir (Dang et

830 al., 2019 and 2020) as well as a groundwater scheme in the model structure.

The WaterGAP2 modeling group plans to update the GRanD dataset used by the model, to include water temperature calculations, to couple the new developed groundwater model (Reinecke et al., 2019), and to update the non-irrigation water use datasets.

The WAYS modeling group plans to develop a new human water use module to consider agricultural, industrial, and domestic

835 water use in the water cycle.

7. Conclusions

Global water models are used to simulate the climate–water–human system. However, recent evaluation studies show that there is a need to better simulate this system by including other hydrological processes, data on physical infrastructure, societal behavior, cultural behavior, water diversions, and virtual water, as well as by identifying its teleconnections on the global scale

840 (Zaherpour et al., 2018; Veldkamp et al., 2018; Wada et al., 2017). These studies also underline the need to better explain various model results.

We undertook the present study mainly to find similarities and differences among global water models that will facilitate interpretation of various results, as well as those of further intercomparison studies. We developed a standard equation writing style to achieve this goal. We found that there are some similarities among the models when applying similar equations for the

845 same hydrological processes; however, model structures are different and various values have been used for parameters or variables or some equations have been adjusted. For example, 10 models (CWatM, DBH, JULES-W1, LPJmL, mHM, ORCHIDEE, PCR-GLOBWB, VIC, WaterGAP2, WAYS) simulate the canopy water storage in a similar way, while 3 models (H08, Mac-PDM.20, and MPI-HM) do not include this compartment. MATSIRO is the only one that has two canopy water compartments: one for rainfall interception and one for snowfall interception. Three models (CLM4.5, CLM5.0, MATSIRO)

850 differentiate between solid and liquid throughfall. Eight global water models (CWatM, LPJmL, Mac-PDM.20, mHM, MPI-HM, PCR-GLOBWB, WaterGAP2, WAYS) use the degree-day method to compute snow accumulation and melt, while six models use the energy balance method (DBH, H08, JULES-W1, ORCHIDEE, MATSIRO, VIC).

Four models (CLM4.5, CLM5.0, JULES-W1, and MATSIRO) use TOPOMODEL for the runoff generation scheme, while three models (CWatM, MPI-HM, and PCR-GLOBWB) use the ARNO model with or without adjustments. Other methods

855 used for runoff generation scheme include Green-Ampt (DBH), Probability Distributed Moisture (Mac-PDM.20), HBV with or without adjustments (mHM and WaterGAP2), XIANJIANG (VIC), bucket (WAYS), Arnold-Bucket (LPJmL), and a leaky bucket (H08).

Three models (H08, WaterGAP2, and WAYS) compute *groundwater recharge* using the same approach described by Döll and Fiedler, 2008. Four models (CWatM, PCR-GLOBWB, WaterGAP2, and WAYS) use the same approach to simulate the

860   *groundwater runoff* by considering it as a part of groundwater storage which is weighted by a groundwater discharge coefficient.

Ten models do not include a lake compartment, while fourteen models do not include a wetland compartment. Four models (CWatM, H08, MATSIRO, and WaterGAP2) include a "global lakes" compartment and "local lakes" compartment in their structure. Furthermore, CWatM, MATSIRO, and WaterGAP2 use the reservoir algorithm developed by H08 modeling group,

865   but with some adjustments. WaterGAP2 also includes a "global wetlands compartment" and "local wetlands compartment". Five models (CWatM, H08, LPJmL, MATSIRO, and WaterGAP2) use a retrospective reservoir algorithm, while one model (PCR-GLOBWB) uses a prospective reservoir algorithm.

Seven models do not simulate human water use sectors (DBH, JULES-W1, Mac-PDM.20, mHM, ORCHIDEE, VIC, and WAYS). Nine models simulate water abstraction for the irrigation sector from surface water bodies (CLM4.5, CLM5.0,

870   CWatM, H08, LPJmL, MATSIRO, MPI-HM, PCR-GLOBWB, WaterGAP2). Additionally, H08, MATSIRO, PCR-GLOBWB, and WaterGAP2 simulate water abstraction for the domestic (household) and manufacturing sectors. Furthermore, WaterGAP2 divides the industry sector in manufacturing and electricity.

Ultimately, in this study and for ISIMIP2b, WaterGAP2 has used the highest number of water storage compartments (11 compartments), while JULES-W1, Mac-PDM.20, and VIC have used the lowest number (3 compartments). CWatM uses 10

875   compartments, while seven models use six compartments (CLM4.5, CLM5.0, LPJmL, H08, mHM, MPI-HM, and PCR-GLOBWB). Two models (CLM4.5 and CLM5.0) have used similar approaches, in most of the cases, because one model (CLM5.0) represents the new extended version of the other (CLM4.5). WaterGAP2 simulates five human water use sectors, while four models (CLM4.5, CLM5.0, LPJmL, and MPI-HM) simulate only water used by humans for the irrigation sector.

We highlight the need to undertake experiments on individual water compartments in order to analyze the equations used and

880   the results obtained. We also underline the need to make multi-model intercomparison projects: firstly, because they enhance collaboration and communication between modeling groups, communities, countries and cultures; secondly, through communication and collaboration, these projects enhance creativity and open opportunities to finding new ways to improve the models. The present study was possible through the international ISIMIP framework.

By improving these models, we can make better decisions on how to use water more efficiently. Therefore, we need to have

885   global water models that develop scenarios regarding how the Earth's water cycle will develop and how it will be affected by climate change. We consider the simulations provided by the ISIMIP2b global water models to represent good hypotheses of our water future and based on them we can make decisions.

Supplement

Tables with equations of each water storage, water flow, human water use sectors, datasets used by global water models,
890   models' structures, future research perspectives.

Acknowledgement

CET and HMS are supported by the German Federal Ministry of Education and Research (grant no. 01LS1711F). We thank
to Jacob Schewe, Agnès Ducharne, Lukas Gudmundsson, and Lamprini Papadimitriou for their useful recommendations on
the manuscript. We also thank to the ISIMIP coordination team for providing funds for ISIMIP2b Global Water Paper-writing
895   Workshop (30 July – 01 August 2018), Frankfurt am Main, Germany and Cross-sectoral ISIMIP Workshop 2019 (04 June
2019), where this manuscript could be discussed as well as to the ISIpedia Stakeholder Engagement Team (Inga Menke,
Quentin Lejeune, Gina Maskell, Kaylin Lee) and ISIpedia stakeholders (Anatolii Shmurak, Atiq Kainan Ahmed, Aimé
Koudou) by providing useful recommendations to create the standard visualization of the water cycle simulated by the models
analyzed in this article. GL is supported by the National Key Research and Development Program of China (No.
900   2020YFA060032) and the National Natural Science Foundation of China (No. 42077420).

Code availability

Information on the availability of source code for the models featured in this article can be found in the Table 12.

Author contributions

CET proposed, designed, and led the conceptualization of ISIMIP2b models' intercomparison based on their water cycle
905   simulation and of a standard writing style of their equations. Initial idea was proposed by HMS, respectively, to compare the
ISIMIP2b models based on their equations and a standard diagram. CET, WT, GL, PB, OR, TS, TT, FH, SR, HMS provided
LaTeX support to write equations on the overleaf platform. HMS, WT, GL, PB, XL, JESB, LPS, MG, YS, OR, TS, JC, NW,
HLS, TT, and GM checked the code and provided models' equations for each water storage and water flow. CET, HMS, WT,
GL, PB, XL, JESB, LPS, MG, YS, OR, TS, JC, NW, HLS, TT, GM, AK, YP, LS, YW, VM, JL, and PD checked the
910   consistency and correctness of the equations. HMS, WT, GL, PB, XL, JESB, LPS, MG, YS, OR, TS, JC, NW, HLS, GM run
simulations for ISIMIP2b project. SNG and HMS coordinated the ISIMIP2b model simulations of the global water sector.
CET conducted the analysis, visualization, and wrote the original draft. All authors reviewed, commented, and contributed to
the final draft.

Competing interests

915 The authors declare that they have no conflict of interest.

References

Abbott, B.W., Bishop K., Zarnetske J.P., Hannah, D. M., Frei1, R. J., Minaudo, C., Stuart, F. C., Krause, S., Conner, L., Ellison, D., Godsey, S. E., Plont, S., Marçais, J., Kolbe, T., Huebner, A., Hampton, T., Gu, S., Buhman, M., Sayedi, S. S., Ursache, O., Chapin, M., Henderson, K. D., and Pinay, G.: A water cycle for the Anthropocene, Hydrological Processes.;1–7.

920 https://doi.org/10.1002/hyp.13544, 2019.

Alcamo, J., Doll, P., Kaspar, F., and Siebert, S.: Global change and global scenarios of water use and availability: An application of WaterGAP 1.0., Rep. A9701, Cent. for Environ. Syst. Res., Univ. of Kassel, Kassel, Germany, 1997.

Arheimer, B., Pimentel, R., Isberg, K., Crochemore, L., Andersson, J. C. M., Hasan, A., and Pineda, L.: Global catchment modelling using World-Wide HYPE (WWH), open data, and stepwise parameter estimation, Hydrol. Earth Syst. Sci., 24, 535–

925 559, https://doi.org/10.5194/hess-24-535-2020, 2020.

Arnell, N. W.: A simple water balance model for the simulation of streamflow over a large geographic domain, J. Hydrol., 217, 314–335, https://doi.org/10.1016/S0022-1694(99)00023-2, 1999.

Arnold, J.G., Williams, J.R., Nicks, A.D. and Sammons, N.B.: SWRRB - A Basin Scale Simulation Model for Soil and Water Resources Management. Texas A&M University Press, College Station, 255pp., 1990.

930 Beck, H. E., van Dijk, A. I. J. M., de Roo, A., Miralles, D. G., McVicar, T. R., Schellekens, J., and Bruijnzeel, L. A., Global-scale regionalization of hydrologic model parameters, Water Resour. Res., 52, 3599–3622, https://doi.org/10.1002/2015WR018247, 2016.

Bergström, S.: Development and application of a conceptual runoff model for Scandinavian catchments, SMHI Report RHO 7, Norrköping, 134, 1976.

935 Best, M. J., Pryor, M., Clark, D. B., Rooney, G. G., Essery, R. L. H., Ménard, C. B., Edwards, J. M., Hendry, M. A., Porson, A., Gedney, N., Mercado, L. M., Sitch, S., Blyth, E., Boucher, O., Cox, P. M., Grimmond, C. S. B., and Harding, R. J.: The Joint UK Land Environment Simulator (JULES), model description – Part 1: Energy and water fluxes, Geosci. Model Dev., 4, 677–699, https://doi.org/10.5194/gmd-4-677-2011, 2011.

Beven, K. J., Kirby, M. J. : A physically based, variable contributing area model of basin hydrology / Un modèle à base

940 physique de zone d'appel variable de l'hydrologie du bassin versant, Hydrological Sciences Journal, 24:1, 43-69, https://doi.org/10.1080/02626667909491834, 1979.

Beven, K: Rainfall-Runoff Modelling – The Primer, 2nd ed, Lancaster University, UK, Wiley-Blackwell, A John Wiley & Sons, Ltd., Plublication, 2012.

Beven, K., and Binley, A.: GLUE: 20 years on, Hydrol. Process. 28, 5897–5918, https://doi.org/10.1002/hyp.10082, 2014.

945   Beven, K., Pappenberger, F. C. H., Lamb, R., and Hunter, N., Hyperresolution information and hyperresolution ignorance in modelling the hydrology of the land surface, Sci. China Earth Sci., 58, 25–35, https://doi.org/10.1007/s11430-014-5003-4, 2015.

Biemans, H., Haddeland, I., Kabat, P., Ludwig, F., Hutjes, R. W. A, Heinke, J., Von Bloh, W., and Gerten, D.: Impact of reservoirs on river discharge and irrigation water supply during the 20th century, Water Resources Research, 47, W03509,
950   https://doi.org/10.1029/2009WR008929W03509, 2011.

Bierkens, M. F. P., Bell, V. A., Burek, P., Chaney, N., Condon, L. E., David, C. H., de Roo, A., Döll, P., Drost, N., Famiglietti, J. S., Flörke, M., Gochis, D. J., Houser, P., Hut, R., Keune, J., Kollet, S., Maxwell, R. M., Reager, J. T., Samaniego, L., Sudicky, E., Sutanudjaja, E. H., van de Giesen, N., Winsemius, H., and Wood, E. F.: Hyper-resolution global hydrological modelling: what is next?, Hydrol. Process., 29, 2, 310–320, https://doi.org/10.1002/hyp.10391, 2015.

955   Bierkens, M.F.P., van Geer, F. C.: Stochastic Hydrology, Department of Physical Geography, Utrecht University, 237, http://www.earthsurfacehydrology.nl/wp-content/uploads/2012/01/Syllabus_Stochastic-Hydrology.pdf, 2007.

Bondeau, A., Pascalle, C. S., Sönke, Z., Schaphoff, S., Lucht, W., Cramer, W., Gerten, D., Lotze-Campen, H., Müller, C., Reichstein, M., Smith, B.: Modelling the role of agriculture for the 20th century global terrestrial carbon balance, Global Change Biology, 13, 679–706, https://doi.org/10.1111/j.1365-2486.2006.01305.x, 2007.

960   Brand, A., Allen, L., Altman, M., Hlava, M., Scott, J.: Beyond authorship: attribution, contribution, collaboration, and credit Beyond authorship: attribution, contribution, collaboration, and credit, Learned Publishing, 28, 2, 151–155, https://doi.org/10.1087/20150211, 2015.

Blöschl G, et al.: Twenty-three Unsolved Problems in Hydrology (UPH) – A community perspective. Hydrological Sciences Journal 64(1):1141–1158. https://doi.org/10.1080/02626667.2019.1620507, 2019.

965   Bouaziz, L. J. E., Thirel, G., de Boer-Euser, T., Melsen, L. A., Buitink, J., Brauer, C. C., De Niel, J., Moustakas, S., Willems, P., Grelier, B., Drogue, G., Fenicia, F., Nossent, J., Pereira, F., Sprokkereef, E., Stam, J., Dewals, B. J., Weerts, A. H., Savenije, H. H. G., and Hrachowitz, M.: Behind the scenes of streamflow model performance, Hydrol. Earth Syst. Sci. Discuss., https://doi.org/10.5194/hess-2020-176, in review, 2020.

Burek, P., Smilovic, M., Satoh, Y., Kahil, T., Guillaumot, L., Tang, T., Greve, P., Wada, Y.: (2019, August 6), Community
970   Water Model (CwatM) (Version v1.04), Zenodo. http://doi.org/10.5281/zenodo.3361478, 2019.

Burek, P., Satoh, Y., Kahil, T., Tang, T., Greve, P., Smilovic, M., Guillaumot, L., Zhao, F., and Wada, Y.: Development of the Community Water Model (CWatM v1.04) - a high-resolution hydrological model for global and regional assessment of integrated water resources management, Geosci. Model Dev., 13, 3267–3298, https://doi.org/10.5194/gmd-13-3267-2020, 2020.

975   Cáceres, D., Marzeion, B., Malles, J. H., Gutknecht, B. D., Müller Schmied, H., and Döll, P.: Assessing global water mass transfers from continents to oceans over the period 1948–2016, Hydrol. Earth Syst. Sci., 24, 4831–4851, https://doi.org/10.5194/hess-24-4831-2020, 2020.

Chow, V. T., Maidment, D. R., and Mays, L. W.: Applied hydrology, McGraw-Hill, New York, 1998.

Clark, D. B., Mercado, L. M., Sitch, S., Jones, C. D., Gedney, N., Best, M. J., Pryor, M., Rooney, G. G., Essery, R. L. H.,
980 Blyth, E., Boucher, O., Harding, R. J., Huntingford, C., and Cox, P. M.: The Joint UK Land Environment Simulator (JULES),
model description – Part 2: Carbon fluxes and vegetation dynamics, Geosci. Model Dev., 4, 701–722,
https://doi.org/10.5194/gmd-4-701-2011, 2011.

CTSM Development Team. (2020, May 1). ESCOMP/CTSM: Update documentation for release-clm5.0 branch, and fix issues
with no-anthro surface dataset creation (Version release-clm5.0.34). Zenodo. http://doi.org/10.5281/zenodo.3779821, 2020.

985 Cuntz, M., J. Mai, L. Samaniego, M. Clark, V. Wulfmeyer, O. Branch, S. Attinger, and S. Thober: The impact of standard and
hard-coded parameters on the hydrologic fluxes in the Noah-MP land surface model, J. Geophys. Res-Atmos, 121(18), 10676–
10700, https://doi.org/10.1002/2016JD025097, 2016.

Dang, T. D., Chowdhury, A. F. M. K., and Galelli, S.: On the representation of water reservoir storage and operations in large-
scale hydrological models: implications on model parameterization and climate change impact assessments, Hydrol. Earth
990 Syst. Sci., 24, 397–416, https://doi.org/10.5194/hess-24-397-2020, 2020.

Dang, T.D., Vu, D.T., Chowdhury, A.F.M.K., and Galelli, S.: A software package for the representation and optimization of
water reservoir operations in the VIC hydrologic model. Environ. Model. SoRw.
https://doi.org/10.1016/j.envsoft.2020.104673, 2020.

Deardorff, J. W.: Efficient prediction of ground surface temperature and moisture, with inclusion of a layer of vegetation, J.
995 Geophys. Res., 83, 1889–1903, https://doi.org/10.1029/JC083iC04p01889, 1978.

Do, H. X., Zhao, F., Westra, S., Leonard, M., Gudmundsson, L., Boulange, J. E. S., Chang, J., Ciais, P., Gerten, D., Gosling,
S. N., Müller Schmied, H., Stacke, T., Telteu, C.-E., and Wada, Y.: Historical and future changes in global flood magnitude –
evidence from a model–observation investigation, Hydrol. Earth Syst. Sci., 24, 1543–1564, https://doi.org/10.5194/hess-24-
1543-2020, 2020.

1000 Dooge, J.: Parameterization of hydrologic processes, in: Proceedings of the Greenbelt Study Conference, edited by: Eagleson,
P., Cambridge University Press, new York, N.Y., 243–288, 1982.

Döll, P., Kaspar, F., and Lehner, B.: A global hydrological model for deriving water availability indicators: model tuning and
validation, Journal of Hydrology, 270, 05–134, https://doi.org/10.1016/S0022-1694(02)00283-4, 2003.

Döll, P., Hoffmann-Dobrev, H., Portmann, F.T., Siebert, S., Eicker, A., Rodell, M., Strassberg, G., and Scanlon, B.R.: Impact
1005 of water withdrawals from groundwater and surface water on continental water storage variations, Journal of Geodynamics,
Volumes 59–60, 143-156, https://doi.org/10.1016/j.jog.2011.05.001, 2012.

Döll, P., Müller Schmied, H., Schuh, C., Portmann, F. T., Eicker, A., Global-scale assessment of groundwater depletion and
related groundwater abstractions: Combining hydrological modelling with information from well observations and GRACE
satellites, Water Resources Research, 50, Issue 7, 5698–5720, https://doi.org/10.1002/2014WR015595, 2014.

1010 Döll, P., Douville, H., Güntner, A., Müller Schmied, H., and Wada, Y.: Modelling Freshwater Resources at the Global Scale:
Challenges and Prospects, Surv. Geophys., 37, 195–221, https://doi.org/10.1007/s10712-015-9343-1, 2016.

Döll, P., and Romero-Lankao, P.: How to embrace uncertainty in participatory climate change risk management—A roadmap, Earth's Future, 5, 18–36, https://doi.org/10.1002/2016EF000411, 2017.

Duan, Q., Schaake, J., Andreassian, V., Franks, S., Goteti, G., Gupta, H. V., Gusev, Y. M., Habets, F., Hall, A., Hay, L., Hogue, T., Huang, M., Leavesley, G., Liang, X., Nasonova, O. N., Noilhan, J., Oudin, L., Sorooshian, S., Wagener, T., and Wood, E. F.: Model parameter estimation experiment (MOPEX): an overview of science strategy and major results from the second and third workshops, J. Hydrol, 320 (1-2), 3-17, https://doi.org/10.1016/j.jhydrol.2005.07.031, 2006.

Dümenil, L., Todini, E.: A rainfall-runoff scheme for use in the Hamburg climate model. In J. P. O'Kane (Ed.), Advances in Theoretical Hydrology: A tribute to James Dooge, Amsterdam: Elsevier Science Publishers B.V., 129-157, http://hdl.handle.net/11858/00-001M-0000-0029-CE00-5, 992.

Duethmann, D., Blöschl, G., and Parajka, J.: Why does a conceptual hydrological model fail to correctly predict discharge changes in response to climate change?, Hydrol. Earth Syst. Sci., 24, 3493–3511, https://doi.org/10.5194/hess-24-3493-2020, 2020.

Ducoudré, N. I., Laval, K. and Perrier, A.: SECHIBA, a New Set of Parameterizations of the Hydrologic Exchanges at the Land-Atmosphere Interface within the LMD Atmospheric General Circulation Model, Journal of Climate, 6(2), 248–273, https://doi.org/10.1175/1520-0442(1993)006<0248:SANSOP>2.0.CO;2, 1993.

Eagleson, P.: The emergence of global-scale hydrology, Water Resour. Res., 22, 6S–14S, https://doi.org/10.1029/WR022i09Sp0006S, 1986.

Eyring, V., Bony, S., Meehl, G. A., Senior, C. A., Stevens, B., Stouffer, R. J., and Taylor, K. E.: Overview of the Coupled Model Intercomparison Project Phase 6 (CMIP6) experimental design and organization, Geosci. Model Dev., 9, 1937-1958, https://doi.org/10.5194/gmd-9-1937-2016, 2016.

Essery, RLH, N Rutter, J Pomeroy, R Baxter, M Staehli, D Gustafsson, A Barr, P Bartlett and K Elder, 2009. SnowMIP2: An evaluation of forest snow process simulations. Bulletin of the American Meteorological Society, 90, 1120 - 1135, https://doi.org/10.1175/2009BAMS2629.1.

Essery, R., Morin, S., Lejeune, Y., and Ménard, C.B.: A comparison of 1701 snow models using observations from an alpine site, Advances in water resources, 55, 131-148, https://doi.org/10.1016/j.advwatres.2012.07.013, 2013.

FAO: Digital Soil Map of the World and derived soil properites (CD-ROM), Land and Water Digital Media Series No 1, http://www.fao.org/geonetwork/srv/en/metadata.show?id=14116, 1995.

Flörke, M., Kynast, E., Bärlund, I., Eisner, S., Wimmer, F., and Alcamo, J.: Domestic and industrial water uses of the past 60 years as a mirror of socio-economic development: A global simulation study, Global Environ. Change, 23, 144–156, https://doi.org/10.1016/j.gloenvcha.2012.10.018, 2013.

Freeze, R. A. and Harlan, R. L: Blueprint for a physically-based, digitally simulated hydrologic response model, J. Hydrol., 9, 237–258, https://doi.org/10.1016/0022-1694(69)90020-1, 1969.

Frieler, K., Lange, S., Piontek, F., Reyer, C. P. O., Schewe, J., Warszawski, L., Zhao, F., Chini, L., Denvil, S., Emanuel, K., Geiger, T., Halladay, K., Hurtt, G., Mengel, M., Murakami, D., Ostberg, S., Popp, A., Riva, R., Stevanovic, M., Suzuki, T.,

Volkholz, J., Burke, E., Ciais, P., Ebi, K., Eddy, T. D., Elliott, J., Galbraith, E., Gosling, S. N., Hattermann, F., Hickler, T., Hinkel, J., Hof, C., Huber, V., Jägermeyr, J., Krysanova, V., Marcé, R., Müller Schmied, H., Mouratiadou, I., Pierson, D., Tittensor, D. P., Vautard, R., van Vliet, M., Biber, M. F., Betts, R. A., Bodirsky, B. L., Deryng, D., Frolking, S., Jones, C. D., Lotze, H. K., Lotze-Campen, H., Sahajpal, R., Thonicke, K., Tian, H., and Yamagata, Y.: Assessing the impacts of 1.5 °C global warming – simulation protocol of the Inter-Sectoral Impact Model Intercomparison Project (ISIMIP2b), Geosci. Model Dev., 10, 4321–4345, https://doi.org/10.5194/gmd-10-4321-2017, 2017.

Gao, H., Tang, Q., Shi, X., Zhu, C., Bohn, T.J., Su, F., Sheffield, J., Pan, M., Lettenmaier, D.P., Wood, E.F.: Water budget record from Variable Infiltration Capacity (VIC) model. Algorithm Theor. Basis Doc. Terr. Water Cycle Data Rec., https://eprints.lancs.ac.uk/id/eprint/89407/1/Gao_et_al_VIC_2014.pdf, 2009.

Gosling, S. N.: Systematic quantification of climate change impacts modelling uncertainty, Impacts World 2013 International Conference on Climate Change Effects (Potsdam: PIK), 268–274, https://gfzpublic.gfz-potsdam.de/rest/items/item_152514_5/component/file_152588/content, 2013.

Gerten, D., Schaphoff, S., Haberlandt, U., Lucht, W., Sitch, S.: Terrestrial vegetation and water balance - hydrological evaluation of a dynamic global vegetation model. Journal of Hydrology, 286(1-4), 249–270, http://dx.doi.org/10.1016/j.jhydrol.2003.09.029, 2004.

Gosling, S. N., Taylor, R. G., Arnell, N. W., and Todd, M. C.: A comparative analysis of projected impacts of climate change on river runoff from global and catchment-scale hydrological models, Hydrol. Earth Syst. Sci., 15, 279–294, https://doi.org/10.5194/hess-15-279-2011, 2011.

Gosling, S. N., Arnell, N. W.: Simulating current global river runoff with a global hydrological model: Model revisions, validation, and sensitivity analysis. Hydrol Processes 25:1129–1145, https://doi.org/10.1002/hyp.7727, 2011.

Greve, P., Kahil, T., Mochizuki, J., Schinko, T., Satoh, Y., Burek, P., Fischer, G., Tramberend, S., Burtscher, R., Langan, S., and Wada, Y.: Global assessment of water challenges under uncertainty in water scarcity projections. Nature Sustainability, 1,486–494, https://doi.org/10.1038/s41893-018-0134-9, 2018.

Greve, P., Burek, P., and Wada, Y.: Using the Budyko Framework for Calibrating a Global Hydrological Model, Water Resources Research, 56 (6), 1-19, e2019WR026280, https://doi.org/10.1029/2019WR026280, 2020.

Grillakis, M.G.: Increase in severe and extreme soil moisture droughts for Europe under climate change, Sci. Total Environ., 660, 1245–1255, https://doi.org/10.1016/j.scitotenv.2019.01.001, 2019.

Guimberteau, M., Ducharne, A., Ciais, P., Boisier, J. P., Peng, S., De Weirdt, M., and Verbeeck, H.: Testing conceptual and physically based soil hydrology schemes against observations for the Amazon Basin, Geosci. Model Dev., 7, 1115–1136, https://doi.org/10.5194/gmd-7-1115-2014, 2014.

Guimberteau, M., Zhu, D., Maignan, F., Huang, Y., Yue, C., Dantec-Nédélec, S., Ottlé, C., Jornet-Puig, A., Bastos, A., Laurent, P., Goll, D., Bowring, S., Chang, J., Guenet, B., Tifafi, M., Peng, S., Krinner, G., Ducharne, A., Wang, F., Wang, T., Wang, X., Wang, Y., Yin, Z., Lauerwald, R., Joetzjer, E., Qiu, C., Kim, H., and Ciais, P.: ORCHIDEE-MICT (v8.4.1), a land surface

model for the high latitudes: model description and validation, Geosci. Model Dev., 11, 121–163, https://doi.org/10.5194/gmd-
1080   11-121-2018, 2018.

Haddeland, I., Clark, D. B., Franssen, W., Ludwig, F., Voß, F., Arnell, N. W., Bertrand, N., Best, M., Folwell, S., Gerten, D.,
Gomes, S., Gosling, S. N., Hagemann, S., Hanasaki, N., Harding, R., Heinke, J., Kabat, P., Koirala, S., Oki, T., Polcher, J.,
Stacke, T., Viterbo, P., Weedon, G. P., Yeh, P.: Multimodel Estimate of the Global Terrestrial Water Balance: Setup and First
Results, Water and Global Change (WATCH) special collection, 869–884, https://doi.org/10.1175/2011JHM1324.1, 2011.

1085   Hagemann, S.: An Improved Land Surface Parameter Dataset for Global and Regional Climate Models, Max-Planck-Institut
für Meteorologie, MPI Report 336, ISSN 0937-1060,
https://mpimet.mpg.de/fileadmin/publikationen/Reports/max_scirep_336.pdf, 2002.

Hagemann, S., Chen, C., Clark, D. B., Folwell, S., Gosling, S. N., Haddeland, I., Hanasaki, N., Heinke, J., Ludwig, F., Voss,
F., and Wiltshire, A. J.: Climate change impact on available water resources obtained using multiple global climate and
1090   hydrology models, Earth Syst. Dynam., 4, 129–144, https://doi.org/10.5194/esd-4-129-2013, 2013.

Hanasaki, N., Kanae, S., and Oki, T.: A reservoir operation scheme for global river routing models, J. Hydrol., 327, 22–41,
https://doi.org/10.1016/j.jhydrol.2005.11.011, 2006 .

Hanasaki, N., Yoshikawa, S., Pokhrel, Y., and Kanae, S.: A global hydrological simulation to specify the sources of water
used by humans, Hydrol. Earth Syst. Sci., 22, 789–817, https://doi.org/10.5194/hess-22-789-2018, 2018.

1095   Hanasaki, N.: (2020, November 8). H08 Version 20190101. Zenodo. http://doi.org/10.5281/zenodo.4263375, 2020.

Hansen, M.C., Sohlberg, R., Defries, R.S., and Townshend, J.R.G.: Global land cover classification at 1 km spatial resolution
using a classification tree approach, Int. J. Remote Sens., 21 (6–7),1331–1364,
https://doi.org/10.1080/014311600210209, 2000.

Hauser, M., Thiery, W., and Seneviratne, S. I.: Potential of global land water recycling to mitigate local temperature extremes,
1100   Earth Syst. Dynam., 10, 157–169, https://doi.org/10.5194/esd-10-157-2019, 2019.

Jones, C. D., Arora, V., Friedlingstein, P., Bopp, L., Brovkin, V., Dunne, J., Graven, H., Hoffman, F., Ilyina, T., John, J. G.,
Jung, M., Kawamiya, M., Koven, C., Pongratz, J., Raddatz, T., Randerson, J. T., and Zaehle, S.: C4MIP – The Coupled
Climate–Carbon Cycle Model Intercomparison Project: experimental protocol for CMIP6, Geosci. Model Dev., 9, 2853-2880,
https://doi.org/10.5194/gmd-9-2853-2016, 2016.

1105   Hirsch, A. L., Wilhelm, M., Davin, E. L., Thiery, W., and Seneviratne, S. I.: Can climate-effective land management reduce
regional warming?, J. Geophys. Res.-Atmos., 122, 2269–2288, https://doi.org/10.1002/2016JD026125, 2017.

Hirsch, A. L., Prestele, R., Davin, E. L., Seneviratne, S. I., Thiery, W., and Verburg, P. H.: Modelled biophysical impacts of
conservation agriculture on local climates, Glob. Change Biol., 24, 4758–4774, https://doi.org/10.1111/gcb.14362, 2018.

Hunger, M. and Döll, P.: Value of river discharge data for global-scale hydrological modelling, Hydrol. Earth Syst. Sci., 12,
1110   841–861, https://doi.org/10.5194/hess-12-841-2008, 2008.

Huss, M. and Hock, R.: Global-scale hydrological response to future glacier mass loss, Nature Climate Change, 8(2), 135-140,
https://doi.org/10.1038/s41558-017-0049-x, 2018.

Jung, M., Reichstein, M., Margolis, H. A., Cescatti, A., Richardson, A. D., Arain, M. A., Arneth, A., Bernhofer, C., Bonal, D., Chen, J., Gianelle, D., Gobron, N., Kiely, G., Kutsch, W., Lasslop, G., Law, B. E., Lindroth, A., Merbold, L., Montagnani, L.,
1115 Moors, E. J., Papale, D., Sottocornola, M., Vaccari, F., and Williams, C.: Global patterns of land-atmosphere fluxes of carbon dioxide, latent heat, and sensible heat derived from eddy covariance, satellite, andmeteorological observations. J. Geophys. Res. 116, G00J07, https://doi.org/10.1029/2010JG001566, 2011.

Kageyama, M., Braconnot, P., Harrison, S. P., Haywood, A. M., Jungclaus, J. H., Otto-Bliesner, B. L., Peterschmitt, J.-Y., Abe-Ouchi, A., Albani, S., Bartlein, P. J., Brierley, C., Crucifix, M., Dolan, A., Fernandez-Donado, L., Fischer, H., Hopcroft,
1120 P. O., Ivanovic, R. F., Lambert, F., Lunt, D. J., Mahowald, N. M., Peltier, W. R., Phipps, S. J., Roche, D. M., Schmidt, G. A., Tarasov, L., Valdes, P. J., Zhang, Q., and Zhou, T.: The PMIP4 contribution to CMIP6 – Part 1: Overview and over-arching analysis plan, Geosci. Model Dev., 11, 1033–1057, https://doi.org/10.5194/gmd-11-1033-2018, 2018.

Kingston, D. G., M. C.Todd, R. G. Taylor, J. R. Thompson, and N. W. Arnell: Uncertainty in the estimation of potential evapotranspirationunder climate change, Geophys. Res. Lett., 36, L20403, https://doi.org/10.1029/2009GL040267, 2009.
1125 Klein Goldewijk, C.G.M. (Utrecht University): Anthropogenic land-use estimates for the Holocene; HYDE 3.2. DANS. https://doi.org/10.17026/dans-25g-gez3, 2017.

Koirala, S., P. J.-F. Yeh, Y. Hirabayashi, S. Kanae, and T. Oki: Global-scale land surface hydrologic modeling with the representation of water table dynamics, J. Geophys. Res. Atmos., 119, 75–89,
 https://doi.org/10.1002/2013JD020398, 2014.
1130 Krysanova, V., Donnelly, C., Gelfan, A., Gerten, D., Arheimer, B., Hattermann, F., and Kundzewicz, Z. W.: How the performance of hydrological models relates to credibility of projections under climate change, Hydro. Scie. J., 63:5, 696–720, https://doi.org/10.1080/02626667.2018.1446214, 2018.

Kundzewicz, Z. W., Krysanova, V., Benestad, R. E., Hov, Ø., Piniewski, M., and Otto, I. M.: Uncertainty in climate change impacts on water resources, Environmental Science and Policy, 79, 1–8, http://dx.doi.org/10.1016/j.envsci.2017.10.008, 2018.
1135 Kumar, R., Samaniego, L. and Attinger, S.: Implications of distributed hydrologic model parameterization on water fluxes at multiple scales and locations. Water Resources Research, 49(1), 360-379, https://doi.org/10.1029/2012WR012195, 2013.

Laloy, E. and Vrugt, J. A.: High-dimensional posterior exploration of hydrologic models using multiple-try DREAM$_{(ZS)}$ and high-performance computing, Water Resour. Res., 48, W01526, https://doi.org/10.1029/2011WR010608, 2012.

Lawrence, D. M., Fisher, R. A., Koven, C. D., Oleson, K. W.,Swenson, S. C., Bonan, G., Collier, N., Ghimire, B., Kampenhout,
1140 L., Kennedy, D., Kluzek, E., Lawrence, P. J., Li, F., Li, H., Lombardozzi, D., Riley, W. J., Sacks, W. J., Shi, M., Vertenstein, M., Wieder, W. R., Xu, C., Ali, A. A., Badger, A. M., Bisht, G., Broeke, M., Brunke, M. A., Burns, S. P., Buzan, J., Clark, M., Craig, A., Dahlin, K., Drewniak, B., Fisher, J. B., Flanner, M., Fox, A. M., Gentine, P., Hoffman, F., KeppelAleks, G., Knox, R., Kumar, S., Lenaerts, J., Leung, L. R., Lipscomb, W. H., Lu, Y., Pandey, A., Pelletier, J. D., Perket, J., Randerson, J. T., Ricciuto, D. M., Sanderson, B. M., Slater, A., Subin, Z. M., Tang, J., Thomas, R. Q., Val Martin, M., and Zeng, X.: The
1145 Community Land Model version 5: Description of new features, benchmarking, and impact of forcing uncertainty, J. Adv. Model. Earth Sy., 2018MS001583, https://doi.org/10.1029/2018MS001583, 2019.

Landerer, F. W., and S. C. Swenson: Accuracy of scaled GRACE terrestrial water storage estimates, Water Resour. Res., 48, W04531, https://doi.org/10.1029/2011WR011453, 2012.

Lehner, B., Verdin, K., and Jarvis, A.: HydroSHEDS Technical Documentation, World Wildlife Fund US, Washington, DC., 26, http://hydrosheds.cr.usgs.gov. 2006.

Lehner, B., Reidy Liermann, C., Revenga, C., Vörösmarty, C., Fekete, B., Crouzet, P., Döll, P., Endejan, M., Frenken, K., Magome, J., Nilsson, C., Robertson, J.C., Rodel, R., Sindorf, N., and Wisser, D.: High-resolution mapping of the world's reservoirs and dams for sustainable river-flow management, Front. Ecol. Environ. 9 494–502, https://doi.org/10.1890/100125, 2011.

Liu, X., Tang, Q., Zhang, X., and Leng, G.: Modeling the Role of Vegetation in Hydrological Responses to Climate Change, In Terrestrial Water Cycle and Climate Change: Natural and Human-Induced Impacts. Hoboken, New Jersey: American Geophysical Union, 193–208, https://doi.org/10.1002/9781118971772.ch10, 2016.

MacBean, N., Scott, R. L., Biederman, J. A., Ottlé, C., Vuichard, N., Ducharne, A., Kolb, T., Dore, S., Litvak, M., and Moore, D. J. P.: Multi-variable, multi-configuration testing of ORCHIDEE land surface model water flux and storage estimates across semi-arid sites in the southwestern US, Hydrol. Earth Syst. Sci. Discuss., https://doi.org/10.5194/hess-2019-598, in review, 2019.

Manabe, S.: Climate and the ocean circulation: The atmospheric circulation and the hydrology of the earth's surface, Mon. Weather Rev., 97, 739–774, https://doi.org/10.1175/1520-0493(1969)097<0739:CATOC>2.3.CO;2, 1969.

Messager, M. L., Lehner, B., Grill, G., Nedeva, I., and Schmitt, O.: Estimating the volume and age of water stored in global lakes using a geo-statistical approach. Nat. Commun., 7, 13603, https://doi.org/10.1038/ncomms13603, 2016.

Mao, G. and Liu, J.: WAYS v1: a hydrological model for root zone water storage simulation on a global scale, Geosci. Model Dev., 12, 5267–5289, https://doi.org/10.5194/gmd-12-5267-2019, 2019.

Mao, G., Liu, J.: (2019, December 17). Water And ecoSYstem Simulator (Version v1.0). Zenodo. http://doi.org/10.5281/zenodo.4255008, 2019.

Masaki, Y., Hanasaki, N., Biemans, H., Müller Schmied, H., Tang, Q., Wada, Y., Gosling, S. N., Takahashi, K. and Hijioka, Y.: Intercomparison of global river discharge simulations focusing on dam operation—multiple models analysis in two case-study river basins, Missouri–Mississippi and Green–Colorado, Environ. Res. Lett. 12, 1–17, https://doi.org/10.1088/1748-9326/aa57a8, 2017.

Meier, R., Davin, E. L., Lejeune, Q., Hauser, M., Li, Y., Martens, B., Schultz, N. M., Sterling, S., and Thiery, W.: Evaluating and improving the Community Land Model's sensitivity to land cover, Biogeosciences, 15 (15), 4731–4757. https://doi.org/10.5194/bg-15-4731-2018, 2018.

Mendoza, P. A., Clark, M. P., Barlage, M., Rajagopalan, B., Samaniego, L., Abramowitz, G., and Gupta, H.: Are we unnecessarily constraining the agility of complex process-based models?, Water Resour. Res., 51(1), 716–728, https://doi.org/10.1002/2014WR015820, 2015.

1180   Milly, P. C. D. and Dunne, K. A: A hydrologic drying bias in water-resource impact analyses of anthropogenic climate change, JAWRA. 53, 822–838, https://doi.org/10.1111/1752-1688.12538, 2017.

Mizuochi, H., Ducharne, A., Cheruy, F., Ghattas, J., Al-Yaari, A., Wigneron, J.-P., Peylin, P., Maignan, F., and Vuichard, N.: Multi-variable evaluation of land surface processes in forced and coupled modes reveals new error sources to the simulated water cycle in the IPSL climate model, Hydrol. Earth Syst. Sci. Discuss., https://doi.org/10.5194/hess-2020-438, in review,
1185   2020.

Moore, R., R. Clarke: A distribution function approach to rainfall runoff modelling, Water Resour. Res., 17(5), 1367–1382, https://doi.org/10.1029/WR017i005p01367, 1981.

Müller Schmied, H., Eisner, S., Franz, D., Wattenbach, M., Portmann, F. T., Flörke, M., and Döll, P.: Sensitivity of simulated global-scale freshwater fluxes and storages to input data, hydrological model structure, human water use and calibration,
1190   Hydrol. Earth Syst. Sci., 18, 3511–3538, https://doi.org/10.5194/hess-18-3511-2014, 2014.

Müller Schmied, H., Adam, L., Eisner, S., Fink, G., Flörke, M., Kim, H., Oki, T., Portmann, F. T., Reinecke, R., Riedel, C., Song, Q., Zhang, J., and Döll, P.: Variations of global and continental water balance components as impacted by climate forcing uncertainty and human water use, Hydrol. Earth Syst. Sci., 20, 2877–2898, https://doi.org/10.5194/hess-20-2877-2016,
2016.

1195   Nazemi, A. and Wheater, H. S.: On inclusion of water resource management in Earth system models – Part 1: Problem definition and representation of water demand, Hydrol. Earth Syst. Sci., 19, 33–61, https://doi.org/10.5194/hess-19-33-2015, 2015.

Nijssen, B., Schnur, R., and Lettenmaier, D.P.: Global retrospective estimation of soil moisture using the variable infiltration capacity land surface model, 1980–93, J. Clim., 14 (8), 1790–1808, https://doi.org/10.1175/1520-
1200   0442(2001)014<1790:GREOSM>2.0.CO;2, 2001.

Oleson, K. W., Lawrence, D. M., Bonan, G. B., Drewniak, B., Huang, M., Koven, C. D., Levis, S., Li, F., Riley, W. J., Subin, Z. M., Swenson, S. C., Thornton, P. E., Bozbiyik, A., Fisher, R., Kluzek, E., Lamarque, J.-F., Lawrence, P. J., Leung, L. R., Lipscomb, W., Muszala, S., Ricciuto, D. M., Sacks, W., Sun, Y., Tang, J., and Yang, Z.-L.: Technical Description of version 4.5 of the Community Land Model (CLM), Ncar Technical Note NCAR/TN-503+STR, National Center for Atmospheric
1205   Research, Boulder, CO, 422 pp., http://dx.doi.org/10.5065/D6RR1W7M, 2013.

Pokhrel, Y., Hanasaki, N., Yeh, P., Yamada, T. J., Shinjiro, K., and Oki, T: Model estimates of sea-level change due to anthropogenic impacts on terrestrial water storage, Nature Geoscience, 5, 389–392,
 https://doi.org/10.1038/ngeo1476, 2012.

Pokhrel, Y. N., Koirala, S., Yeh, P. J.-F., Hanasaki, N., Longuevergne, L., Kanae, S., and T. Oki: Incorporation of groundwater
1210   pumping in a global Land Surface Model with the representation of human impacts, Water Resour. Res., 51, 78–96, https://doi.org/10.1002/2014WR015602, 2015.

Portmann, F. T., Siebert, S., Döll, P.: MIRCA2000—Global monthly irrigated and rainfed crop areas around the year 2000: A new high-resolution data set for agricultural and hydrological modeling, Global Biogeochemical Cycles, 24, GB1011, https://doi.org/10.1029/2008GB003435, 2010.

1215 Prudhomme, Ch., Giuntoli, I., Robinson, E. L., Clark, D. B., Arnell, N. W., Dankers, R., Fekete, B. M., Franssen, W., Gerten, D., Gosling, S. N., Hagemann, S., Hannah, D. M., Kim, H., Masaki, Y., Satoh, Y., Stacke, T., Wada, Y., and Wisser, D.: Hydrological droughts in the 21st century, hotspots and uncertainties from a global multimodel ensemble experiment, PNAS, 111, 9, 3262–3267, doi/10.1073/pnas.1222473110, 2014.

Rabin, S. S., Melton, J. R., Lasslop, G., Bachelet, D., Forrest, M., Hantson, S., Kaplan, J. O., Li, F., Mangeon, S., Ward, D.
1220 S., Yue, C., Arora, V. K., Hickler, T., Kloster, S., Knorr, W., Nieradzik, L., Spessa, A., Folberth, G. A., Schaphoff, S., Heyder, U., Ostberg, S., Gerten, D., Heinke, J., and Lucht, W.: Contribution of permafrost soils to the global carbon budget, Environ. Res. Lett. 8, 014026, https://doi.org/10.1088/1748-9326/8/1/014026, 2013.

Rost, S., Gerten, D., Bondeau, A., Lucht, W., Rohwer, J., Schaphoff, S.: Agricultural green and blue water consumption and its influence on the global water system. Water Resources Research, 44, W09405, doi:
1225 http://dx.doi.org/10.1029/2007WR006331, 2008.

Schaphoff, S., von Bloh, W., Rammig, A., Thonicke, K., Biemans, H., Forkel, M., Gerten, D., Heinke, J., Jägermeyr, J., Knauer, J., Langerwisch, F., Lucht, W., Müller, C., Rolinski, S., and Waha, K.: LPJmL4 – a dynamic global vegetation model with managed land – Part 1: Model description, Geosci. Model Dev., 11, 1343–1375, https://doi.org/10.5194/gmd-11-1343-2018, 2018.

1230 Sheehan, T., Voulgarakis, A., Kelley, D. I., Prentice, I. C., Sitch, S., Harrison, S., and Arneth, A.: The Fire Modelling Intercomparison Project (FireMIP), phase 1: experimental and analytical protocols with detailed model descriptions, Geosci. Model Dev., 10, 1175–1197, https://doi.org/10.5194/gmd-10-1175-2017, 2017.

Reinecke, R., Müller Schmied, H., Trautmann, T., Burek, P., Flörke, M., Gosling, S. N., Grillakis, M., Hanasaki, N., Koutroulis, A., Pokhrel, Y., Seaby, L., Thiery, W., Wada, Y., Yusuke, S., and Döll, P.: Uncertainty of simulated groundwater
1235 recharge at different global warming levels: A global-scale multi-model ensemble study, Hydrol. Earth Syst. Sci. Discuss., https://doi.org/10.5194/hess-2020-235, in review, 2020.

Richards, L. A., Capillary conduction of liquids through porous mediums, Journal of Applied Physics, 1 (5), https://doi.org/10.1063/1.1745010, 1931.

Scanlon, B. R., Zhang, Z., Rateb, A., Sun, A., Wiese, D., Save, H., Beaudoing, H., Lo, M. H., Müller-Schmied, H., Döll, P.,
1240 van Beek, R., Swenson, S., Lawrence, D., Croteau, M., and Reedy, R. C.: Tracking seasonal fluctuations in land water storage using global models and GRACE satellites. Geophysical Research Letters, 46, 5254–5264, https://doi.org/10.1029/2018GL081836, 2019.

Samaniego, L., Kumar, R., Mai, J., Zink, M., Thober, S., Cuntz, M., Rakovec, O., Schäfer, D., Schrön, M., Brenner, J., Demirel, C. M., Kaluza, M., Langenberg, B., Stisen, S., Attinger, S.: (2017, December 1). mesoscale Hydrologic Model
1245 (Version v5.8). Zenodo. http://doi.org/10.5281/zenodo.1069203, 2007.

Samaniego, L., Kumar, R., and Attinger, S.: Multiscale parameter regionalization of a grid-based hydrologic model at the mesoscale, Water Resour. Res., 46, 1–25, https://doi.org/10.1029/2008WR007327, 2010.

Samaniego, L., Kumar, R., Thober, S., Rakovec, O., Zink, M., Wanders, N., Eisner, S., Müller Schmied, H., Sutanudjaja, E. H., Warrach-Sagi, K., and Attinger, S.: Toward seamless hydrologic predictions across spatial scales, Hydrol. Earth Syst. Sci., 21, 4323–4346, https://doi.org/10.5194/hess-21-4323-2017, 2017.

Shah, H., Mishra, V., (2020, November 5). Varibale Infiltration Capacity (VIC) Model for ISIMIP2B (Global Water Sector) (Version Version 4.1.2.g). Zenodo. http://doi.org/10.5281/zenodo.4247673, 2020.

Sutanudjaja, E., van Beek, R., Wanders, N., Wada, Y., Bosmans, J., Drost, N., van der Ent, R., de Graaf, I., Hoch, J., de Jong, K., Karssenberg, D., López López, P., Peßenteiner, S., Schmitz, O., Straatsma, M., Vannametee, E., Wisser, D., Bierkens, M.: PCR-GLOBWB 2 input files version 2017_11_beta_1 (Version v_2017_11_beta_1) [Data set], Zenodo. http://doi.org/10.5281/zenodo.1045339, 2017.

Sutanudjaja, E. H., van Beek, R., Wanders, N., Wada, Y., Bosmans, J. H. C., Drost, N., van der Ent, R. J., de Graaf, I. E. M., Hoch, J. M., de Jong, K., Karssenberg, D., López López, P., Peßenteiner, S., Schmitz, O., Straatsma, M. W., Vannametee, E., Wisser, D., and Bierkens, M. F. P.: PCR-GLOBWB 2: a 5 arcmin global hydrological and water resources model, Geosci. Model Dev., 11, 2429–2453, https://doi.org/10.5194/gmd-11-2429-2018, 2018.

Sausen, R., Schubert, S., and Dümenil, L.: A model of river runoff for use in coupled atmosphere-ocean models, Journal of Hydrology, 155, (3–4), 337-352, https://doi.org/10.1016/0022-1694(94)90177-5, 1994.

Schellnhuber, H. J., Frieler, K., and Kabat, P.: The elephant, the blind, and the intersectoral intercomparison of climate impacts, PNAS, March 4, 111 (9), 3225–3227; https://doi.org/10.1073/pnas.1321791111, 2014.

Schewe, J., Heinke, J., Gerten, D., Haddeland, I., Arnell, N.W., Clark, D.B., Dankers, R., Eisner, S., Fekete, B., Colón-González, F.J., Gosling, S.,N., Kim, H., Liu, X., Masaki, Y, Portmann, F.T., Satoh, Y., Stacke, T., Tang, Q., Wada, Y., Wisser, D., Albrecht, T., Frieler, K., Piontek, F., Warszawski, L., Kabat, P.: Multi-model assessment of water scarcity under climate change, Proceedings of the National Acadamy of Sciences 111, https://doi.org/10.1073/pnas.1222460110, 2014.

Schewe, J., Gosling, S. N., Reyer, Ch., Zhao, F., Ciais, Ph., Elliott, J., Francois, L., Huber, V., Lotze, H. K., Seneviratne, S. I., van Vliet, M. T. H., Vautard, R., Wada, Y., Breuer, L., Büchner, M., Carozza, D. A., Chang, J., Coll, M., Deryng, D., de Wit, A., Eddy, T. D., Folberth, Ch., Frieler, K., Friend, A. D., Gerten, D., Gudmundsson, L., Hanasaki, N., Ito, A., Khabarov, N., Kim, H., Lawrence, P., Morfopoulos, C., Müller, Ch., Müller Schmied, H., Orth, R., Ostberg, S., Pokhrel, Y., Pugh, T. A. M., Sakurai, G., Satoh, Y., Schmid, E., Stacke, T., Steenbeek, J., Steinkamp, J., Tang, Q., Tian, H., Tittensor, D. P., Volkholz, J., Wang, X., and Warszawski L.: State-of-the-art global models underestimate impacts from climate extremes, Nat. Comm., 10, 1–14, https://doi.org/10.1038/s41467-019-08745-6, 2019.

Schrapffer, A., Sörensson, A., Polcher, J. and Fita, L.: Benefits of representing floodplains in a Land Surface Model: Pantanal simulated with ORCHIDEE CMIP6 version. Climate Dynamics, 55, 1303–1323, https://doi.org/10.1007/s00382-020-05324-0, 2020.

Shah, H.L., Zhou, T., Huang, M., and Mishra, V.: Strong influence of irrigation on water budget and land surface

1280 temperature in Indian sub-continental river basins. J. Geophys. Res. Atmos. https://doi.org/10.1029/2018JD029132, 2019a.

Shah, H.L., Zhou, T., Sun, N., Huang, M., and Mishra, V.: Roles of irrigation and reservoir operations in modulating terrestrial water and energy budgets in the Indian Subcontnental River Basins. J. Geophys. Res. Atmos. 124, 12915–12936. https://doi.org/10.1029/2019JD031059, 2019b.

Smith, K. A.: Investigating uncertainty in global hydrology modelling. PhD thesis, University of Nottingham.
1285 http://eprints.nottingham.ac.uk/31875/, 2016.

Stacke, T. and Hagemann, S.: Development and evaluation of a global dynamical wetlands extent scheme, Hydrol. Earth Syst. Sci., 16, 2915–2933, https://doi.org/10.5194/hess-16-2915-2012, 2012.

Sultan, B., Lejeune, Q., Menke, I., Maskell, G., Lee, K., Noblet, M., Sy I., and Roudier, P.: Current needs for climate services in West Africa: Results from two stakeholder surveys, Climate Services, 18, 1-14,
1290 https://doi.org/10.1016/j.cliser.2020.100166, 2020.

Takata, K., S. Emori, and T. Watanabe: Development of the minimal advanced treatments of surface interaction and runoff. Global Planet. Change, 38, 209–222, https://doi.org/10.1016/S0921-8181(03)00030-4, 2003.

Tang, Q., T. Oki, and Kanae, S.: A distributed biosphere hydrological model (DBHM) for large river basin. Ann. J. Hydraul. Eng. JSCE, 50, 37–42, https://doi.org/10.2208/prohe.50.37, 2006.

1295 Tang, Q., Rosenberg, E. A., and Lettenmaier, D. P.: Use of satellite data to assess the impacts of irrigation withdrawals on Upper Klamath Lake, Oregon. Hydrology and Earth System Sciences, 13(5), 617–627. https://doi.org/10.5194/hess-13-617-2009, 2009.

Thiery, W., E. L. Davin, D. M. Lawrence, A. L. Hirsch, M. Hauser, and S. I. Seneviratne: Present-day irrigation mitigates heat extremes, J. Geophys. Res. Atmos., 122, 1403–1422, https://doi.org/10.1002/2016JD025740, 2017.

1300 Thiery, W., Visser, A.J., Fischer, E.M., Hauser, M., Hirsch, A. L., Lawrence, D. M., Lejeune, Q., Davin, E. L., Seneviratne, S. I.: Warming of hot extremes alleviated by expanding irrigation, Nat Commun 11, 290, https://doi.org/10.1038/s41467-019-14075-4, 2020 a.

Thiery, W., Visser, A. J., Fischer, E. M., Hauser, M., Hirsch, A. L., Lawrence, D. M., Lejeune, Q., Davin, E. L., and Seneviratne, S. I.: Warming of hot extremes alleviated by expanding irrigation. Nat Commun 11, 290 (2020).
1305 https://doi.org/10.1038/s41467-019-14075-4, 2020 b.

Thiery, W. (user, not author). (2020, November 17). CESM1.2.2_CLM4.5_freeze_ISIMIP2b (Version CESM1.2.2 - CLM4.5). Zenodo. http://doi.org/10.5281/zenodo.4277137, 2020.

Thober, S., Cuntz, M., Kelbling, M., Kumar, R., Mai, J., and Samaniego, L.: The multiscale routing model mRM v1.0: simple river routing at resolutions from 1 to 50 km, Geosci. Model Dev., 12, 2501–2521, https://doi.org/10.5194/gmd-12-2501-2019,
1310 2019.

Ullrich, P. A., Jablonowski, C., Kent, J., Lauritzen, P. H., Nair, R., Reed, K. A., Zarzycki, C. M., Hall, D. M., Dazlich, D., Heikes, R., Konor, C., Randall, D., Dubos, T., Meurdesoif, Y., Chen, X., Harris, L., Kühnlein, C., Lee, V., Qaddouri, A., Girard, C., Giorgetta, M., Reinert, D., Klemp, J., Park, S.-H., Skamarock, W., Miura, H., Ohno, T., Yoshida, R., Walko, R.,

Reinecke, A., and Viner, K.: DCMIP2016: a review of non-hydrostatic dynamical core design and intercomparison of
1315   participating models, Geosci. Model Dev., 10, 4477-4509, https://doi.org/10.5194/gmd-10-4477-2017, 2017.

University Corporation for Atmospheric Research (UCAR) – National Center for Atmospheric Research (NCAR). The
Community Earth System Model version 1.2.2 (CESM1.2). Subversion Code Repository. https://svn-ccsm-
models.cgd.ucar.edu/cesm1/release_tags/cesm1_2_2/.

Veldkamp, T. I. E., Zhao, F., Ward, P. J., de Moel, H., Aerts, J. C. J. H., Müller Schmied, H., Portmann, F. T., Masaki, Y.,
1320   Pokhrel, Y., Liu, X., Satoh, Y., Gerten, D., Gosling, S. N., Zaherpour, J., and Wada, Y.: Human impact parameterizations in
global hydrological models improve estimates of monthly discharges and hydrological extremes: a multi-model validation
study, Environ. Res. Lett., 13, 1–7, https://doi.org/10.1088/1748-9326/aab96f, 2018.

Wada, Y., van Beek, L. P. H., Viviroli, D., Weingartner, R., Bierkens, M. F. P.: Global monthly water stress: 2. Water demand
and severity of water stress, Water Resources research, 47, W07518, 1–17, https://doi.org/10.1029/2010WR009792, 2011.

1325   Wada, Y., van Beek, L. P. H., Wanders, N., and Bierkens, M. F.P.: Human water consumption intensifies hydrological drought
worldwide, Environ. Res. Lett., 8, 034036, doi:10.1088/1748-9326/8/3/034036, 2013a.

Wada, Y., Wisser, D., Eisner, S., Flörke, M., Gerten, D., Haddeland,I., Hanasaki, N., Masaki, Y., Portmann, F. T., Stacke, T.,
Tessler,Z., and Schewe, J.: Multimodel projections and uncertainties of irrigation water demand under climate change,
Geophys. Res.Lett., 40, 4626–4632, https://doi.org/10.1002/grl.50686, 2013b.

1330   Wada, Y., D. Wisser, and Bierkens, M. F. P.: Global modelling of withdrawal, allocation and consumptive use of surface water
and groundwater resources, Earth Syst. Dynam., 5, 15-40, https://doi.org/10.5194/esd-5-15-2014, 2014.

Wada, Y., Flörke, M., Hanasaki, N., Eisner, S., Fischer, G., Tramberend, S., Satoh, Y., van Vliet, M. T. H., Yillia, P., Ringler,
C., Burek, P., and Wiberg, D.: Modelling global water use for the 21st century: the Water Futures and Solutions (WFaS)
initiative and its approaches, Geosci. Model Dev., 9, 175–222, https://doi.org/10.5194/gmd-9-175-2016, 2016a.

1335   Wada, Y., de Graaf, I. E. M., and van Beek, L. P. H.: High-resolution modelling of human and climate impacts on global water
resources, J. Adv. Model Earth Sy., 8, 735–763, https://doi.org/10.1002/2015MS000618, 2016b.

Wada, Y., Bierkens, M. F. P., de Roo, A., Dirmeyer, P. A., Famiglietti, J. S., Hanasaki, N., Konar, M., Liu, J., Müller Schmied,
H., Oki, T., Pokhrel, Y., Sivapalan, M., Troy, T. J., van Dijk, A. I. J. M., van Emmerik, T., Van Huijgevoort, M. H. J., Van
Lanen, H. A. J., Vörösmarty, C. J., Wanders, N., and Wheater, H.: Human–water interface in hydrological modelling: current
1340   status and future directions, Hydrol. Earth Syst. Sci., 21, 4169–4193, https://doi.org/10.5194/hess-21-4169-2017, 2017.

Vanderkelen, I., van Lipzig, N.P.M., Lawrence, D.M., Droppers, B., Golub, M., Gosling, S.N., Janssen, A.B.G., Marce, R.,
Schmied, H.M., Perroud, M. and Pierson, D., Pokhrel, Y., Satoh, Y., Schewe, J., Seneviratne, S. I., Stepanenko, V. M., Tan,
Z., Woolway, R. I., and Thiery, W.: Global heat uptake by inland waters, Geophysical Research Letters, 47, 1-10,
https://doi.org/10.1029/2020GL087867, 2020.

1345   Van Beek, L. P. H., Wada, Y., Bierkens, M. F. P.L: Global monthly water stress: 1. Water balance and water availability,
Water Resour. Res., 47, W07517, https://doi.org/10.1029/2010WR009791, 2011.

von Lampe, M., Willenbockel, D., Ahammad, H., Blanc, E., Cai, Y., Calvin, K., Fujimori, S., Hasegawa, T., Havlik, P., Heyhoe, E., Kyle, P., Lotze-Campen, H., Mason d'Croz, D., Nelson, G.C., Sands, R.D., Schmitz, C., Tabeau, A., Valin, H., van der Mensbrugghe, D., van Meijl, H.: Why do global long-term scenarios for agriculture differ? An overview of the AgMIP
1350   global economic model intercomparison. Agric. Econ. 45, 3–20, https://doi.org/10.1111/agec.12086, 2014.

Verbeke, T., Tootchi, A., Jost, A., Ghattas, J., Cheruy, F. and Ducharne, A.: Subgrid-scale parametrization of groundwater-soil moisture interactions in the ORCHIDEE land surface model: first results at global scale. In Geophysical Research Abstracts (Vol. 21), https://meetingorganizer.copernicus.org/EGU2019/EGU2019-16650.pdf, 2019.

Verzano, K., Bärlund, I., Flörke, M., Lehner, B., Kynast, E., Voß, F., and Alcamo, J.: Modeling variable river flow velocity
1355   on continental scale: current situation and climate change impacts in Europe, J. Hydrol., 424-425, 238–251, https://doi.org/10.1016/j.jhydrol.2012.01.005, 2012.

Vörösmarty, C. J., Federer, C. A., and A. Schloss: Potential evaporation functions compared on US watersheds: Implications for global-scale water balance and terrestrial ecosystem modelling, J. Hydrol., 207, 147–169, https://doi.org/10.1016/S0022-1694(98)00109-7, 1998.

1360   Vörösmarty, C. J., Fekete, B. M., Meybeck, M., and Lammers, R. B.: Global system of rivers: Its role in organizing continental land mass and defining land-To-Ocean linkages, Global Biogeochem. Cy., 14, 599–621, https://doi.org/10.1029/1999GB900092, 2000.

Wagener, T., Gleeson, T., Coxon, G., Hartmann, A., Howden, N., Pianosi, F., Rahman, M., Rosolem, R., Stein, L., Woods, R.: On doing large-scale hydrology with Lions: Realising the value of perceptual models and knowledge accumulation,
1365   EarthArXiv, https://doi.org/10.31223/osf.io/zdy5n, in review, 2020.

Wang, C., Duan, Q., Charles, H. T., Zhenhua, D., and Gong, W.: A GUI platform for uncertainty quantification of complex dynamical models, Environmental Modelling & Software, 76, 1–12, http://dx.doi.org/10.1016/j.envsoft.2015.11.004, 2016.

Warszawski, L., Frieler, K., Huber, V., Piontek, F., Olivia Serdeczny, Jacob Schewe: The Inter-Sectoral Impact Model Intercomparison Project (ISI–MIP): Project framework Proceedings of the National Academy of Sciences Mar 2014, 111 (9)
1370   3228–3232; https://doi.org/10.1073/pnas.1312330110, 2014.

Wartenburger, R., Seneviratne, S. I., Hirschi, M., Chang, J., Ciais, P., Deryng, D., Elliott, J., Folberth, C., Gosling,S.N., Gudmundsson, L., Henrot, A.-J., Hickler, T., Ito, A., Khabarov, N., Kim, H., Leng, G., Liu, J., Liu, X., Masaki, Y., Morfopoulos, C., Müller, C., Müller Schmied, H., Nishina, K., Orth, R., Pokhrel, Y., Pugh, T.A.M., Satoh, Y., Schaphoff, S., Schmid, E., Sheffield, J., Stacke, T., Steinkamp, J., Tang, Q., Thiery, W., Wada, Y., Wang, X., Weedon, G. P., Yang, H., Zhou,
1375   T.: Evapotranspiration simulations in ISIMIP2a—Evaluation of spatio-temporal characteristics with a comprehensive ensemble of independent datasets, Environmental Research Letters, 13, 075001, doi: 10.1088/1748-9326/aac4bb, 2018.

Wisser, D., Fekete, B. M., Vörösmarty, C. J., and Schumann, A. H.: Reconstructing 20th century global hydrography: a contribution to the Global Terrestrial Network- Hydrology (GTN-H), Hydrol. Earth Syst. Sci., 14, 1–24, https://doi.org/10.5194/hess14-1-2010, 2010.

1380 Wood, E. F., Roundy, J. K., Troy, T. J., van Beek, L. P. H., Bierkens, M. F. P., Blyth, E., de Roo, A., Döll, P., Ek, M., Famiglietti, J., Gochis, D., van de Giesen, N., Houser, P., Jaffé, P. R., Kollet, S., Lehner, B., Lettenmaier, D. P., Peters-Lidard, C., Sivapalan, M., Sheffield, J., Wade, A., and Whitehead, P.: Hyperresolution global land surface modelling: Meeting a grand challenge for monitoring Earth's terrestrial water, Water Resour. Res., 47, W05301, https://doi.org/10.1029/2010WR010090, 2011.

1385 Yeh, P. J. F., and E. A. B. Eltahir: Representation of water table dynamics in a land surface scheme. Part I: Model development, J. Clim., 18, 1861–1880, https://doi.org/10.1175/JCLI3330.1, 2005.

Yin, Z., Wang, X. H., Ottlé, C., Zhou, F., Guimberteau, M., Polcher, J., Peng, S. S., Piao, S. L., Li, L., Bo, Y., and Chen, X. L.: Improvement of the irrigation scheme in the ORCHIDEE land surface model and impacts of irrigation on regional water budgets over China. Journal of Advances in Modeling Earth Systems, 12(4), https://doi.org/10.1029/2019MS001770, 2020.

1390 Zaherpour, J., Gosling, S. N., Mount, N., Müller Schmied, H., Veldkamp, T. I. E., Dankers, R., Eisner, S., Gerten, D., Gudmundsson, L., Haddeland, I., Hanasaki, N., Kim, H., Leng, G., Liu, J., Masaki, Y., Oki, T., Pokhrel, Y., Satoh, Y., Schewe, Ja., and Wada, Y.: Worldwide evaluation of mean and extreme runoff from six global-scale hydrological models that account for human impacts, Environ. Res. Lett., 13, 1–18, 065015, https://doi.org/10.1088/1748-9326/aac547, 2018.

Zaherpour, J., Mount, N., Gosling, S.N., Dankers, R., Eisner, S., Gerten, D., Liu, X., Masaki, Y., Müller Schmied, H., Tang,
1395 Q. and Wada, Y.: Exploring the value of machine learning for weighted multi-model combination of an ensemble of global hydrological models. Environmental modelling & software, 114, 112-128, https://doi.org/10.1016/j.envsoft.2019.01.003, 2019.

Zhao, R.-J., Zhuang, Y. L., Fang, L. R., Liu, X. R., and Zhang, Q. S.: The Xinanjiang model. In: Hydrological Forecasting, Proceedings of the Oxford Symposium, April 1980. IAHS Publ. No. 129. 1980.

1400 Zekollari, H., Huss, M., and Farinotti, D.: Modelling the future evolution of glaciers in the European Alps under the EURO-CORDEX RCM ensemble, The Cryosphere, 13, 1125–1146, https://doi.org/10.5194/tc-13-1125-2019, 2019.

Table 1: Canopy compartment and its water flows included in ISIMIP2b Global Water Models

Canopy water storage (S_{ca}) (Tables S3 – S7): CLM4.5, CLM5.0, CWatM, DBH, JULES-W1, LPJmL, mHM, MATSIRO, ORCHIDEE, PCR-GLOBWB, VIC, WaterGAP2, WAYS.
Inflows: - total precipitation (P) (sum of rainfall and snowfall, as input data): CWatM, DBH, JULES-W, LPJmL, mHM, ORCHIDEE, PCR-GLOBWB, VIC, WaterGAP2, WAYS.   - rainfall (P_{ra}) (as input data): CLM4.5, CLM5.0, MATSIRO.   - snowfall (P_{sn}) (as input data): CLM4.5, CLM5.0, MATSIRO. - precipitation intercepted by canopy storage: CLM4.5, CLM5.0, CWatM, DBH, Mac-PDM.20, MATSIRO, mHM, WaterGAP2, WAYS. **Outflows:** - evaporation of the water intercepted by canopy or interception loss or canopy evaporation (E_{ca}): CLM4.5, CLM5.0, CWatM, DBH, JULES-W1, LPJmL, mHM, MATSIRO, ORCHIDEE, PCR-GLOBWB, VIC, WaterGAP2, WAYS. -precipitation falls directly to the ground: CLM4.5, CLM5.0, H08, VIC. - throughfall (P_{th}): CLM4.5, CLM5.0, CWatM, DBH, JULES-W1, LPJmL, MATSIRO mHM, ORCHIDEE, PCR-GLOBWB, VIC, WaterGAP2, WAYS.

1405

Table 2: Snow and soil compartments and their water flows included in ISIMIP2b Global Water Models

Snow storage (S_{sn}) (Tables S8 – S13): CLM4.5, CLM5.0, CWatM, DBH, H08, JULES-W1, LPJmL, Mac-PDM.20, mHM, MATSIRO, MPI-HM, ORCHIDEE, PCR-GLOBWB, VIC, WaterGAP2, WAYS.
- snow held on the canopy (S_{soc}): CLM5.0, DBH, JULES-W1, MATSIRO, VIC.
- snow under the canopy (S_{suc}): CLM5.0, DBH, JULES-W1, MATSIRO, ORCHIDEE, VIC.

Inflows:
-total precipitation (P_{tot}): DBH, CWatM, JULES-W1, WaterGAP2.
- snowfall (P_{sn}): CLM4.5, CLM5.0, H08, Mac-PDM.20, MATSIRO, mHM, MPI-HM, PCR-GLOBWB, WAYS.
-throughfall (P_{th}): LPJmL.
-snowfall and rainfall: ORCHIDEE, VIC.

Outflows:
- sublimation (E_{sn}): CLM4.5, CLM5.0, CWatM, DBH, H08, JULES-W1, LPJmL, MATSIRO, ORCHIDEE, VIC, WaterGAP2.
- snowmelt (M): CLM4.5, CLM5.0, CWatM, DBH, H08, JULES-W1, LPJmL, Mac-PDM.20, mHM, MATSIRO, MPI-HM, ORCHIDEE, PCR-GLOBWB, VIC, WaterGAP2, WAYS.

Soil storage (S_{so}) (Tables S14 – S25): CLM4.5, CLM5.0, CWatM, DBH, H08, JULES-W1, LPJmL, Mac-PDM.20, mHM, MATSIRO, MPI-HM, ORCHIDEE, PCR-GLOBWB, VIC, WaterGAP2, WAYS.

Inflows:
-total precipitation (P_{tot}): Mac-PDM.20
- infiltration (R_{in}): CWatM, DBH, H08, LPJmL, mHM, MPI-HM, ORCHIDEE, PCR-GLOBWB, WaterGAP2,.
-throughfall (P_{th}): JULES-W1, WAYS.
-snowmelt (M): JULES-W1, Mac-PDM.20, WAYS.
- capillary rise (R_{cr}): CWatM.

Outflows:
- transpiration (T): CLM4.5, CLM5.0, CWatM, DBH, LPJmL, MPI-HM, PCR-GLOBWB.
- evaporation from soil (E_{so}): CWatM, DBH, H08, JULES-W1, LPJmL, Mac-PDM.20, mHM, MPI-HM, ORCHIDEE, PCR-GLOBWB, WaterGAP2, WAYS.
- surface runoff (R_{su}): JULES-W1, Mac-PDM.20, ORCHIDEE.
- interflow (R_{if}): CWatM, JULES-W1, LPJmL, PCR-GLOBWB.
- groundwater recharge (R_{gwr}): CWatM, DBH, MATSIRO, PCR-GLOBWB.

1410

1415

1420 **Table 3: Groundwater, lake, reservoir, and wetland compartments and their water flows included in ISIMIP2b Global Water Models**

Groundwater storage (S_{gw}) (Table S26-S28): CLM4.5, CLM5.0, CWatM, H08, Mac-PDM.20, mHM, MATSIRO, MPI-HM, PCR-GLOBWB, WaterGAP2, WAYS.

Inflows:
- groundwater recharge (R_{gwr}): CLM4.5, CLM5.0, H08, Mac-PDM.20, mHM, MPI-HM, WaterGAP2, WAYS.
- percolation (R_{pe}): CWatM, PCR-GLOBWB.
- preferential flow (Q_{pf}): CWatM.

Outflows:
- capillary rise (R_{cr}): CWatM, PCR-GLOBWB.
- groundwater runoff (R_{gw}): CLM4.5, CLM5.0, CWatM, H08, Mac-PDM.20, mHM, MPI-HM, PCR-GLOBWB, WaterGAP2, WAYS.
- groundwater withdrawal for human water use (A_{gw}): PCR-GLOBWB, WaterGAP2.
- total human water abstraction (A_{tot}): H08.

Lake (S_{la}) (Tables S29-S31): CLM4.5, CLM5.0, CWatM, LPJmL, PCR-GLOBWB, WaterGAP2.

Inflows:
- precipitation (P_{tot}): LPJmL, WaterGAP2
- inflow from upstream surface water bodies (Q_{iu}): LPJmL, WaterGAP2
- groundwater runoff (R_{gw}): WaterGAP2
- return flow from human water use (A_{rf}): WaterGAP2
- water abstraction for human purposes: LPJmL

Outflows:
- evaporation from lake (E_{la}): LPJmL, PCR-GLOBWB, WaterGAP2
- outflow from lake (Q_{la}): LPJmL, PCR-GLOBWB, WaterGAP2
- groundwater recharge (R_{gwr}): WaterGAP2
- water abstraction for human water use from lake (A_{la}): WaterGAP2, LPJmL

Reservoir storage (S_{re}) (Tables S32-S35): DBH, H08, LPJmL, MATSIRO, PCR-GLOBWB, WaterGAP2.

Inflows:
- precipitation (P_{tot}): WaterGAP2, LPJmL
- inflow from upstream surface water bodies (Q_{iu}): CWatM, PCR-GLOBWB, WaterGAP2.
- total runoff (R_{tot}): H08, MATSIRO
- groundwater recharge below surface water bodies (R_{gwr}^{swb}): WaterGAP2
- return flow from human water use (A_{rf}): LPJmL, MATSIRO, PCR-GLOBWB, WaterGAP2

Outflows:
- evaporation from reservoir (E_{re}): WaterGAP2, CLM4.5, CLM5.0, LPJmL, VIC.
- outflow from reservoir (Q_{re}): DBH, H08, LPJmL, MATSIRO, PCR-GLOBWB, WaterGAP2.
- groundwater recharge (R_{gwr}): WaterGAP2.
- water abstraction for human water use from reservoir (A_{re}): LPJmL, H08, MATSIRO, PCR-GLOBWB, WaterGAP2.

Wetland storage (S_{we}) (Tables S36-S39): MPI-HM, WaterGAP2.

Inflows:
- precipitation (P): MPI-HM, WaterGAP2
- inflow from upstream surface water bodies (Q_{iu}): MPI-HM, WaterGAP2

Outflows:
- groundwater recharge (R_{gwr}): WaterGAP2
- evaporation from wetland (E_{we}): MPI-HM, WaterGAP2
- outflow from wetland (Q_{we}): MPI-HM, WaterGAP2

Table 4: River compartment and its water flows included in the ISIMIP2b Global water Models

River storage (S_{ri}) (Tables S40-S45): CLM4.5, CLM5.0, CWatM, DBH, H08, LPJmL, mHM, MATSIRO, MPI-HM, ORCHIDEE, PCR-GLOBWB, WaterGAP2, WAYS.
Inflows: - inflow from upstream surface water bodies (Q_{iu}): CLM4.5, CLM5.0, CWatM, H08, LPJmL, mHM, MATSIRO, PCR-GLOBWB, WaterGAP2. -total runoff (R_{tot}): mHM - surface runoff or overland flow or fast runoff (R_{su}): CLM4.5, CLM5.0, CWatM, ORCHIDEE, PCR-GLOBWB, WaterGAP2. - interflow (R_{if}): CWatM, PCR-GLOBWB - groundwater runoff (R_{gw}): CLM4.5, CLM5.0, CWatM, H08, mHM, MATSIRO, MPI-HM, ORCHIDEE, PCR-GLOBWB, WaterGAP2. - return flow from human water use (A_{rf}): WaterGAP2 . - streamflow (Q_{ri}): H08, MPI-HM **Outflows:** - streamflow or outflow or river discharge (Q_{ri}): CLM4.5, CLM5.0, LPJmL, mHM, MPI-HM, WaterGAP2 - inflow upstream of a grid cell (Q_{iu}): H08 - mean total annual inflow in a lake ($Q_{iu,la}$): LPJmL - outflow downstream of a grid cell (Q_{od}): CWatM, PCR-GLOBWB - water abstraction for irrigation (A_{irr}): LPJmL, - water abstraction for irrigation from surface water bodies (A_{irr}^{sw}): CWatM, PCR-GLOBWB - water abstraction for domestic sector from surface water bodies (A_{dom}^{sw}): CWatM, PCR-GLOBWB - water abstraction for livestock from surface water bodies (A_{liv}^{sw}): CWatM, PCR-GLOBWB - water abstraction for manufacturing from surface water bodies (A_{man}^{sw}): CWatM, PCR-GLOBWB - water abstraction for human water use from river (A_{ri}): WaterGAP2, H08, MATSIRO - water abstraction for irrigation sector (A_{irr}): LPJmL

1425

Table 5: Human water use sectors estimated by ISIMIP2b GWMs

Human water use sectors (A) (Tables S40-S80): Irrigation (A_{irr}): CLM4.5, CLM5.0, CWatM, H08, LPJmL, MATSIRO, MPI-HM, PCR-GLOBWB, WaterGAP2. Domestic (A_{dom}): MATSIRO, PCR-GLOBWB, WaterGAP2, CWatM Manufacturing (A_{man}): MATSIRO, PCR-GLOBWB, WaterGAP2, CWatM Electricity (A_{ele}): PCR-GLOBWB, WaterGAP2, CWatM Livestock (A_{liv}): CWatM, PCR-GLOBWB, WaterGAP2.

Table 6: Key characteristics of the Global Water Models

Model	Model Type	Temporal resolution	Discretization Type	Calibration / Ability to calibrate / Details	Human water use sectors
CLM4.5	LSM	6 hours	grid, subgrid for vegetation, surface runoff, and evapotranspiration	no / no, adjustment of some parameters according to vegetation or soil properties / not available	sim A_{irr}
CLM5.0	LSM	6 hours	grid, subgrid for vegetation, surface runoff, and evapotranspiration	no / yes / calibration performed in a Bayesian framework based on sequential Monte Carlo	sim A_{irr}
CWatM	GHM	1 day	grid, subgrid for land cover, snow	yes, calibrated for 12 catchment / monthly or daily discharge / hydrological calibration uses DEAP (Burek et al., 2020)	sim: A_{irr}, A_{dom}, A_{nd}, A_{liv}
DBH	LSM	1 day	grid	no / no hydrological calibration, adjustment of some parameters according to vegetation or soil properties / most parameters derived from satellite data.	not included
H08	GHM	1 day	grid	no / can be calibrated but generally done at the regional scale / the model can be applied at the global or regional scale	sim A_{irr} and A^{ocean}, A_{dom}, A_{ind}, A^{ocean}
JULES-W1	LSM	1 day	grid	biophysical processes are calibrated / no hydrologic calibration / ✖	not included
LPJmL	DGVM	1 day	grid	yield calibration to match FAO stats / no hydrological calibration	sim A_{irr}, ISIMIP2b prescribed A_{dom} and A_{ind}
Mac-PDM.20	GHM	1 day	grid	no / yes / calibration uses a 100,000 GLUE ensemble with WATCH Forcing Data (Smith, 2016)	not included
MATSIRO	LSM	1 hour	grid	no / yes / adjustment of some parameters according to vegetation or soil properties, no calibration capability in TRIP model for routing discharge.	sim A_{irr}, ISIMIP2b prescribed A_{dom} and A_{ind}
mHM	GHM	1 day	grid	yes / yes / calibration is performed against observed daily discharge GRDC stations, gridded fields of TWS and gridded ET from FLUXNET with the ERA5 climate forcing	not included
MPI-HM	GHM	1 day	grid, subgrid for surface runoff and evapotranspiration	no / ✖ / ✖	sim A_{irr}
ORCHIDEE	LSM	30 min	grid	no / yes / adjustment of some parameters	not included
PCR-GLOBWB	GHM	1 day	grid, subgrid for vegetation, land cover	no / yes / adjustment of some parameters	sim: A_{irr}, A_{dom}, A_{ind}, A_{liv}, A_{ocean}
VIC	GHM	1 day	grid, subgrid for vegetation and elevation	no calibration for ISIMIP2b	not included
WaterGAP2	GHM	1 day	grid, subgrid for snow	yes / mean annual discharge / Beta function, 1319 GRDC stations	sim: A_{irr}, A_{dom}, A_{man}, A_{elec}, A_{liv}
WAYS	GHM	1 day	grid	yes / yes / calibrated against the ISLSCP, Initiative II UNH or GRDC composite monthly runoff data (Fekete et al., 2011) from 1986 to 1995 at a 0.5°resolution	not included

Legend: ✖ = no details; DEAP = Distributed Evolutionary Algorithms in Python; DGVM = dynamic global vegetation model; EB = energy balance; GHM = global hydrological model; GRDC = Global Runoff Data Centre; ISLSCP = International Satellite Land Surface Climatology Project; LSM = land surface model; sim = simulated by the model; UNH = University of New Hampshire; A_{irr} = water abstractions for irrigation; A_{dom} = water abstractions for domestic; A_{man} = water abstractions for manufacturing; A_{ele} = water abstractions for cooling of thermal power plants; A_{ind} = water abstractions for industry (sum of A_{man} and A_{ele}); A_{liv} = water abstractions for livestock; TRIP = Total Runoff Integrating Pathways; **Bold** = LSMs; *Italic* = GHMs; Underline = DGVMs.

Table 7: Representation of the water storages and water flows included in the Global Water Models – PART I

Model	Interception scheme	Vegetation scheme Partition / Photosynthesis scheme	(Potential) evapotranspiration scheme	Number of soil layers	Soil scheme Soil layer depth SLD [m]	TSD [m]	Snow scheme Snow accumulation and snowmelt	Snow$_{acc}$
CLM4.5	f(LAI, SAI)	tile approach with 24 PFTs (including 10 crop types) / ✖; CO$_2$	Monin-Obukhov Similarity Theory computes only AET	15	depth at layer interface: 0.0175, 0.0451, 0.0906, 0.1655, 0.2891, 0.4929, 0.8289, 1.3828, 2.2961, 3.8019, 6.2845, 10.3775, 17.1259, 28.2520, 42.1032.	42.1	physically based snow module	5 layers
CLM5.0	f(LAI, SAI)	naturally vegetated surfaces are comprised of up to 14 possible plant functional types (PFTs) / dynamic global vegetation model (DGVM); CO$_2$	Monin-Obukhov Similarity Theory computes only AET	25, f(depth to bedrock)	depth at layer interface: 0.020; 0.060; 0.120; 0.200; 0.320; 0.480; 0.680; 0.920; 1.200; 1.520; 1.880; 2.280; 2.720; 3.260; 3.900; 4.640; 5.480; 6.420; 7.460; 8.600; 10.990; 15.666; 23.301; 34.441; 49.556.	49.6	physically based snow module	maximum 12 layers, depends on snow depth
CWatM	f(veg)	subgrid	Penman-Monteith	3	0.05,0.05-0.3, 0.3-1.7 depends on HWSD data	2.0	Degree-day Method	7 layers
DBH	f(LAI)	prescribed, 10 vegetation types (PFTs) with fixed vegetation characteristics / ✖	Energy balance model with Monin-Obukhov similarity theory computes only AET	3	from 1.5 to 3.5m; top layer = 0.020m; root layer = 1.0 to 1.5m.	3.5	Energy Balance Method	1 layer
H08	✖	tile approach / ✖	Bulk, Bulk transfer coefficient set to 0.003	1 / RCZ	1	1	Energy Balance Method	1
JULES-W1	f(LAI)	5 static vegetation types (PFTs) with fixed plant characteristic / ✖	Penman-Monteith	4	0.10; 0.25; 0.65; 2.00	3.0	Energy Balance Method	zero-layer scheme
LPJmL	f(LAI)	9 PFTs f(L, W, S) / DVPNV; CO$_2$	Priestley-Taylor modified for transpiration	5+1	0.20; 0.30; 0.50; 1; 1m. 1 thermally active soil of 10m	13	Degree-day Method with precipitation factor	1 layer
Mac-PDM.20	f(veg)	prescribed, 16 PFTs with fixed vegetation characteristics / ✖	Penman-Monteith	1	none	none	Degree-day Method	1 layer
MATSIRO	f(LAI)	11 static vegetation types with fixed characteristics (PFTs) / ✖	Monin-Obukhov Similarity Theory, to compute only actual evapotranspiration	13	0.05; 0.2; 0.75; 1; 1; 1; 1; 1; 1; 1; 1; 1; 90m.	100	Energy Balance Method	3 layers

Legend: AET = actual evapotranspiration; CO$_2$ = CO$_2$ fertilization effect; DGVM = dynamic global vegetation model; DVPNV = dynamic vegetation composition on potential natural vegetation areas; f(LAI) = function of leaf area index; f(LAI, SAI) = function of leaf area index (LAI) and stem area index (SAI); f(veg) = function of vegetation type; HWSD = Harmonized World Soil Database (FAO et al., 2012: http://www.fao.org/soils-portal/soil-survey/soil-maps-and-databases/harmonized-world-soil-database-v12/en/); L= light; PFTs = Plant functional types; RCZ = runoff properties varies with climate zones; SLD = soil layers depth from top to bottom; TSD = total soil layer depth; Snow$_{acc}$ = snow accumulation; S = space; W = water; ✖ = not included in the model; **Bold** = LSMs; *Italic* = GHMs; Underline = DGVMs.

Table 8: Representation of the water storages and water flows included in the Global Water Models – PART II

Model	Interception scheme	Vegetation scheme Partition / Photosynthesis scheme	(Potential) evapotranspiration scheme	Number of soil layers	Soil scheme Soil layer depth SLD [m]	TSD [m]	Snow scheme Snow accumulation and snowmelt	Snow$_{acc}$
mHM	f(veg)	3 major vegetation classes: (forest, impervious, pervious) for parameter regionalization + long-term dynamics based on LAI-based on GIMMS	Hargreaves-Samani	6	soil layers correspond to SoilGrids250 vertical discretizaion, i.e.: 0-5cm, 5-15cm, 15-30cm,30-50cm, 50-100cm,100-200cm	2.0	Degree-day Method	1 layer
MPI-HM	✘	prescribed, Land Surface Parameter dataset 2 / ✘	Penman-Monteith reference Evapotranspiration	1, f(FC)	none	none	Degree-day Method	1 layer
ORCHIDEE	f(LAI)	tile approach with 17 vegetation types (PFTs); CO_2	Penman & Monteith (Monteith, 1965) based on the correction term developed by Chris Milly (1992)	11	0.001; 0.003; 0.006; 0.012; 0.023; 0.047; 0.094; 0.188; 0.375; 0.750; 0.500.	2	Energy Balance Method	3 layers
PCR-GLOBWB	f(veg)	natural vegetation (short and tall vegetation) and agriculture (rainfed, rice irrigated and non-rice irrigated) prescribed annually by HYDE dataset and MIRCA, GLOBCOVER / ✘	Hamon	2	variable up from 0 to 0.3 (first layer) and variable from 0.3 to 1.5 (second layer)	1.5	Degree-day Method	1 layer
VIC	f(veg)	any number of vegetation types with fixed characteristics can be represented (PFTs) / ✘	Penman-Monteith	3	variable, first layer is fixed to 0.1-0.3m, second and third layers are calibrated	6.15	Energy Balance Method	variable
WaterGAP2	f(LAI)	LAI development model based on T and P / ✘	Priestley-Taylor with varying alpha-values for arid and humid areas	1	from 0.1 to 4m	4	Degree-day Method	SG
WAYS	f(LAI)	14 static vegetation types (PFTs) with fixed characteristics / ✘	Penman-Monteith	1/the complete root zone	variable, derived separately from remote sensing data	variable	Degree-day Method	1

Legend: AET = actual evapotranspiration; CO_2 = CO_2 fertilization effect; f(LAI) = function of leaf area index; f(veg) = function of vegetation type; f(FC) = function of field capacity; P = precipitation; PFTs = Plant functional types; SG = subgrid; SLD = soil layers depth from top to bottom; TSD = total soil layer depth; Snow$_{acc}$ = snow accumulation; T = subgrid temperature (daily average) (0° C); ✘ = not included in the model; **Bold** = LSMs; *Italic* = GHMs.

Table 9: Representation of the water storages and water fluxes included in the Global Water Models – PART III

Model	Groundwater scheme / groundwater layer	Runoff generation scheme surface runoff / subsurface runoff	River scheme / River routing[1] / flow velocity[2] / floodplain scheme / Details	Reservoir scheme / reservoir operation / Number / Details	Lakes scheme / Details	Wetlands scheme / Details
CLM4.5	✓ / 1	TOPMODEL[Beven and Kirkby,1979] / R_{ho}, R_{sat} / f(gw)	✓ / River Transport Model (RTM) / 0.35 m s^{-1} RtM / ✗ / diagnostic tool, conserves water globally	✗	virtual storage / constant lake depth	✗
CLM5.0	✓ / 1	TOPMODEL[Beven and Kirkby,1979] / R_{ho}, R_{sat} / f(gw)	✓ / MOSART / based on Manning's equation / ✗ / MOSART based on kinematic wave method	✗	virtual storage / spatially variable depth	✗
CWatM	✓ / 1	ARNO[Dümenil and Todini, 1992] / R_{sat} / f(soil and gw)	✓ / Kinematic wave, approximation of the Saint-Venant equation[Chow et al., 1998] / variable Manning-Strickler equation / ✗ / linear storage	✓ / ✓ / 3663, HydroLakes[3]/ retrospective: following H08: Hanasaki et al. (2018) and Wisser et al. (2010).	✓ / Modified Puls	✗
DBH	✗ / ✗	Green-Ampt method/ R_{ho} / ✗	✗/ ✗/ ✗ / ✗ / ✗ /.	✗/ ✗/ ✗	✗	✗
H08	✓ / 1 renewable and 1 nonrenewable gw layer	leaky Bucket[Manabe,1969] / R_{sat} / f(soil) RCZ	✓ / based on 30' flow drainage direction map (DDM30) / 0.5 m s^{-1} / ✗ / Rfd	✓ / ✓/ 963 global reservoirs and 5824 local reservoirs / retrospective: Hanasaki et al., 2006	✗	✗
JULES-W1	seepage as gw recharge and gw runoff / ✗	TOPMODEL[Beven and Kirkby,1979] / R_{ho}, R_{sat} / f(gw)	✗ / ✗ / ✗ / ✗ / ✗	✗	✗	✗
LPJmL	seepage as gw recharge and gw runoff / ✗	Bucket[Arnold et al., 1990]/ R_{sat} / f(soil)	✓ / continuity equation derived from linear reservoir model / 1 m s^{-1} / ✗ / linear storage buffer; Rfd	✓ / ✓ / 4134, GRanD / retrospective: Biemans et al., 2011	✓	✗
Mac-PDM.20	✗ / 1	Probability Distributed Moisture (PDM)[Moore and Clarke,1981] / Rsat / f(gw)	✗ / ✗ / ✗ / ✗ / ✗	✗	✗	✗
MATSIRO	✓ Dgws / ~13	TOPMODEL[Beven and Kirkby,1979] / R_{ho}, R_{sat} / f(soil)	✓ / linear reservoir, TRIP / 0.5 m s^{-1} / ✗ / ✗ TRIP	✓ / ✓ / 728 global reservoirs and 6134 'local reservoirs' / following H08, retrospective: Pokhrel et al., 2012	✗	✗

Legend: ✓ = included in the model; ✗ = not included in the model for ISIMIP2b simualtions; Dgws = dynamic groundwater scheme; GRanD = Global Reservoir and Dam database according to Lehner et al., 2011; gw = groundwater; R_{su} = surface runoff; R_{sat} = R_{su} modelled as saturation excess overland flow; R_{ho} = R_{su} modelled as infiltration excess or hortonian overland flow; f(gw) = subsurface flow or interflow modelled as a function of groundwater; f(soil) = subsurface flow or interflow modelled as a function of soil moisture (soil); Rfd = the model routes runoff along flow direction; RtM = routing model; TRIP = Total Runoff Integrating Pathways; **Bold** = LSMs; *Italic* = GHMs; Underline = DGVMs.
Notes: 1: Data source: www.isimip.org. **2:** Zhao et al., 2017. **3:** CWatM, HydroLakes database: Messager et al., 2016; Lehner et al., 2011.

Table 10: Representation of the water storages and water fluxes included in the Global Water Models – PART IV

Model	Groundwater scheme / groundwater layer	Runoff generation scheme surface runoff / subsurface runoff	River scheme / River routing[1] / flow velocity[2] / floodplain scheme / Details	Reservoir scheme / reservoir operation / Number / Details	Lakes scheme / Details	Wetlands scheme / Details
mHM	✘ / 1	HBV[Bergström,1976] + VIC 3Layers / R_{sat} / f(soil)	✔ / mesoscale Routing Model with adaptive timestep, spatially varying celerity[3] / ✘ / ✘/ ✘	✘	✘	✘
MPI-HM	✘ / 1	ARNO[Dümenil and Todini, 1992] / R_{sat} / *f*(soil)	✔ / linear reservoir cascade / variable, Manning-Strickler Equation / ✔ / RtMwefp	✘		lake storage is part of the wetland storage
ORCHIDEE	✘/ ✘	SECHIBA[Ducoudré et al., 1993] / R_{ho} / *f*(soil)	✔/ STN-30p river network / variable, Manning-Strickler Equation / ✔ / wetlands act as floodplains	✘	✘	✘ / wetlands act as floodplains
PCR-GLOBWB	✔ / 1	ARNO[Dümenil and Todini, 1992] / R_{sat} / *f*(soil and gw)	✔/ travel time routing (characteristic distance) linked with dynamic reservoir operation / variable based on channel dimension and Manning-Strickler Equation / ✔ / ✘	✔ / ✔ / 6862: GRanD / prospective: Wada et al., 2014	✘	✘
VIC	✘ / ✘ / seepage as gw recharge and gw runoff / ✘	XIANJIANG [Zhao, 1980] / R_{sat} / *f*(soil)	✘/ ✘/ ✘ / ✘ / ✘	✘	✘	✘
WaterGAP2	✔ / 1	HBV[Bergström,1976] / R_{sat}, Beta function / ✘	✔ / linear reservoir cascade / variable, Manning-Strickler Equation / ✘ / ✘	✔ / ✔ / 11097: GRanD / retrospective, following H08: Döll et al, 2009	✔ / local and global lakes[4]	✔/ local and global wetlands[5]
WAYS	✔ / 1	Bucket[Manabe,1969]/ Beta function[3] / f(soil)	✘ / ✘ / ✘ / ✘ / ✘	✘	✘	✘

Legend: ✔= included in the model; ✘ = not included in the model for ISIMIP2b simualtions; GRanD = Global Reservoir and Dam database according to Lehner et al., 2011; gw = groundwater; R_{su} = surface runoff; R_{sat} = R_{su} modelled as saturation excess overland flow; R_{ho} = R_{su} modelled as infiltration excess or hortonian overland flow; *f*(gw) = subsurface flow or interflow modelled as a function of groundwater; *f*(soil) = subsurface flow or interflow modelled as a function of soil moisture (soil); RtMwefp = routing model with wetlands (we) and floodplain (fp) scheme; **Bold** = LSMs; *Italic* = GHMs.
Notes: **1:** Data source: www.isimip.org. **2:** Zhao et al., 2017. **3:** Thober et al, 2019; **4 and 5: WaterGAP2**, Döll et al., 2012.

Table 11 Challenges of global hydrological modelling overlapping with unsolved problems in hydrology

	Challenges of hydrological modelling
Time variability and change (Blöschl et al., 2019)	**Challenges of simulating terrestrial water cycle on the global scale, identified through the present study**
1. Is the hydrological cycle regionally accelerating/decelerating under climate and environmental change, and are there tipping points (irreversible changes)? 2. How will cold region runoff and groundwater change in a warmer climate (e.g. with glacier melt and permafrost thaw)? 3. What are the mechanisms by which climate change and water use alter ephemeral rivers and groundwater in (semi-) arid regions?	**a.** couple the climate and hydrological models, having climate feedback from the hydrological models (Ning et al., 2019); **b.** add glacial meltwater runoff (Schewe et al., 2019; Huss and Hock, 2018, Zekollari et al., 2019; Cáceres et al., 2020); **c.** couple the climate, lands use, hydrology, and human components including their feedbacks and interactions (Nazemi &Wheater, 2015; Pokhrel et al., 2016; Wada et al., 2017; Thiery et al., 2017; 2020); **d.** land-use dynamics scheme (Sood and Smakhtin, 2015)
Measurements and data (Blöschl et al., 2019)	**Challenges of simulating terrestrial water cycle on the global scale, identified through the present study**
16. How can we use innovative technologies to measure surface and subsurface properties, states, and fluxes at a range of spatial and temporal scales? 18. How can we extract information from available data on human and water systems in order to inform the building process of socio-hydrological models and conceptualizations?	**e.** perform the GWMs at a high resolution of 1 km than 55 km (Wood et al., 2011; Bierkens 2015; Beven et al., 2015; Wada et al., 2016b; Burek et al., 2020); **f.** improve the quality of the input data, GRACE products (Murray et al., 2012; Scanlon et al., 2018); **g.** make single-model sensitivity analyses (Gosling and Arnell, 2011; Müller Schmied et al. 2014; Pianosi et al., 2015; Cuntz et al., 2016); **h.** make multi-parameterization of the single models or model compartments; **j.** improve the simulation of the human impact on freshwater resources (Bierkens, 2015; Nazemi&Wheater, 2015; Döll et al., 2016; Wada et al., 2017; Masaki et al., 2017; Veldkamp et al., 2018); **i.** distinguish between the groundwater source and surface water source for water abstractions and identify how the return flows recharge groundwater (Döll et al., 2016; Veldkamp et al., 2018; Scanlon et al., 2019).
Modelling methods (Blöschl et al., 2019)	**Challenges of simulating terrestrial water cycle on the global scale, identified through the present study**
19. How can hydrological models be adapted to be able to extrapolate to changing conditions, including changing vegetation dynamics? 20. How can we disentangle and reduce model structural/parameter/input uncertainty in hydrological prediction?	**k.** understand different model biases (errors) and their influence on the simulations identify and explain the strengths and weaknesses of individual models (fire community: Rabin et al., 2017); **l.** assess the influence of the models' structure on simulations, go deep into equations, to improve the equations, and to create new equations; **m.** improve the processes representation of the models, for example, incorporation of a dynamic groundwater scheme (Pokhrel et al., 2016; Scanlon et al., 2019); **n.** add other processes in the models such as transmission losses, capillary rise, evaporation from small ephemeral ponds, dynamic response of vegetation to the climate change and CO_2 concentrations; improve the capture of the spatial pattern, intra and inter-annual variabilities; explain the reasons for different output results and use several types of data (e. g., GRACE, GPS, well observations, MODIS, Envisat) for multi-criteria validation (of the models' outputs), model calibration (models' parameters), data assimilation (Döll et al., 2003; Döll et al., 2015; Döll et al., 2016; Vanderkelen et al., 2020); **o.** improve parameterizations by using parameter transfer method, multiscale parameter regionalization (Samaniego et al., 2010), or by using stepwise parameter estimation (Arheimer et al., 2020); **p.** add floodplain storage and wetland evaporation; to develop or open new data sets on "interbasin transfers, regional water distribution network, river cross-sectional dimensions, and hydrogeological subsurface properties" (Bierkens, 2015, page 4942); **q.** weight individual models based upon their performance (Zaherpour et al., 2019) **r.** identify hidden parameters in the code (Mendosa et al., 2015)
Interfaces with society (Blöschl et al., 2019)	**Challenges of simulating terrestrial water cycle on the global scale, identified through the present study**
21. How can the (un)certainty in hydrological predictions be communicated to decision makers and the general public? 22. What are the synergies and tradeoffs between societal goals related to water management (e.g. water–environment–energy–food–health)? 23. What is the role of water in migration, urbanisation and the dynamics of human civilisations, and what are the implications for contemporary water management?	**s.** evaluate the models' performance, for example, following the steps proposed by Krysanova et al., 2018 or to create new feasible steps for GWMs taking into account their shortcomings (Zaherpour et al., 2018 and 2019) or evaluating them for several scales and gauge stations (Samaniego et al., 2017); **t.** compare with the outputs of the high-resolution continental scale models (for example, Parflow) (Scanlon et al., 2018); **u.** complement the global studies with regional studies (Gosling et al., 2011; Gosling et al., 2017; Hatterman et al., 2017); **v.** connect the GWMs with socio-economic and energy models (Calvin et al., 2013; Burek et al., 2020); **x.** identify and explain the strengths and weaknesses of multi-model ensembles, individual model compartments (Clark et al., 2011; Niu et al., 2011; Essery et al., 2013);
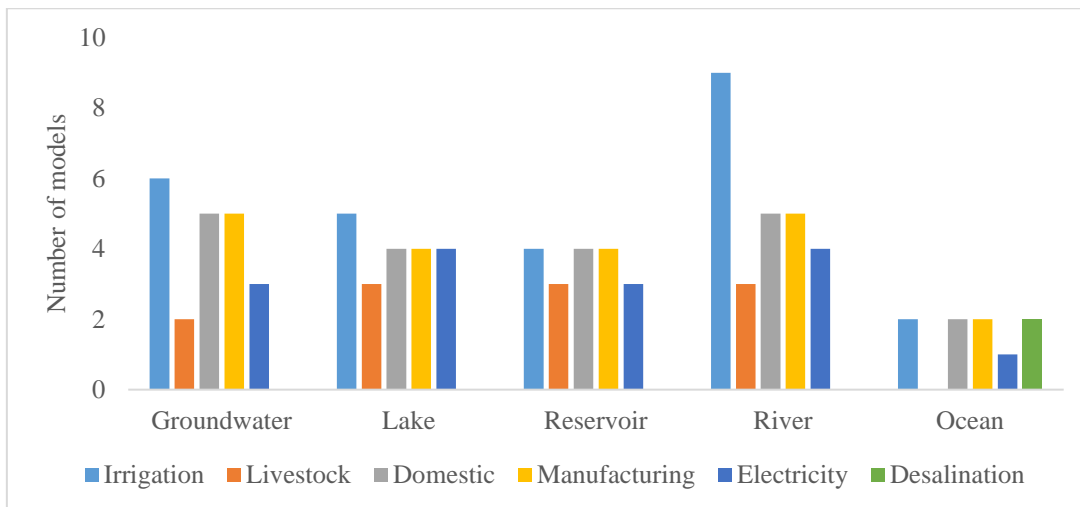
Figure 1: Number of global water models that consider water source for human water use sectors
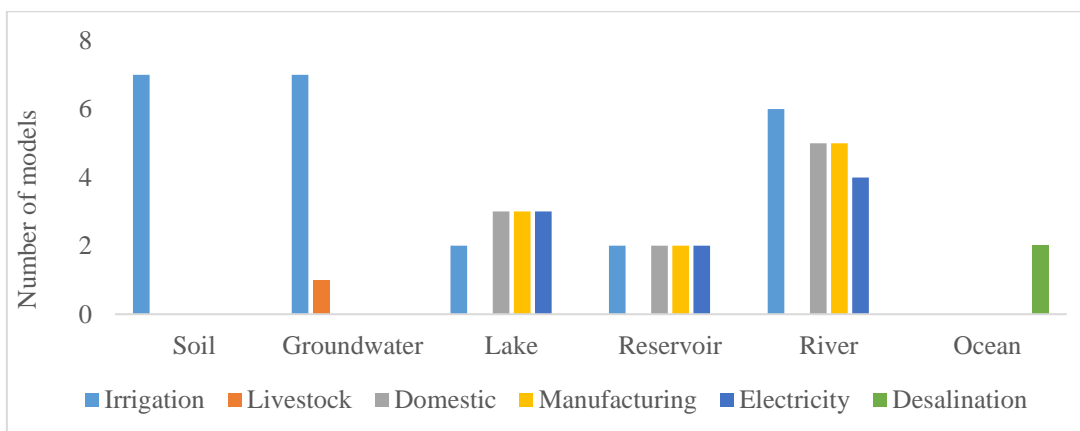
Figure 2: Number of global water models that consider return flow destination
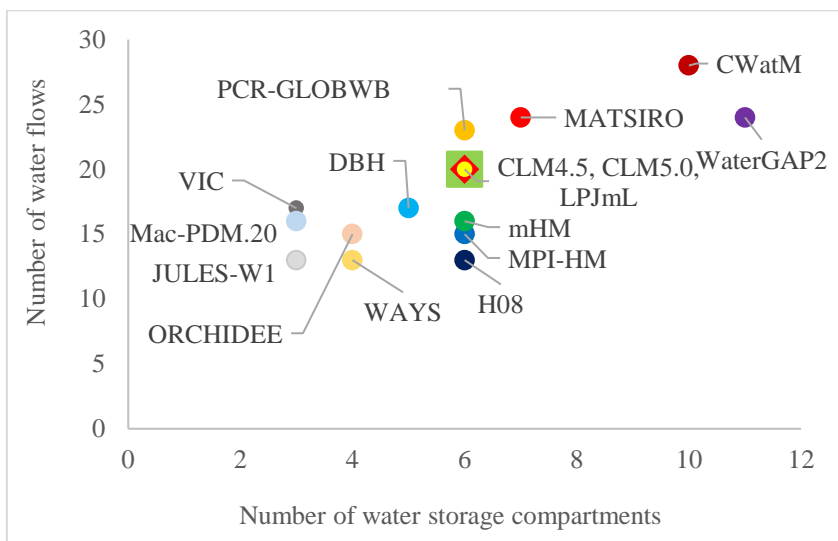
Figure 3: Number of water storage compartments and water flows included in the global water models.
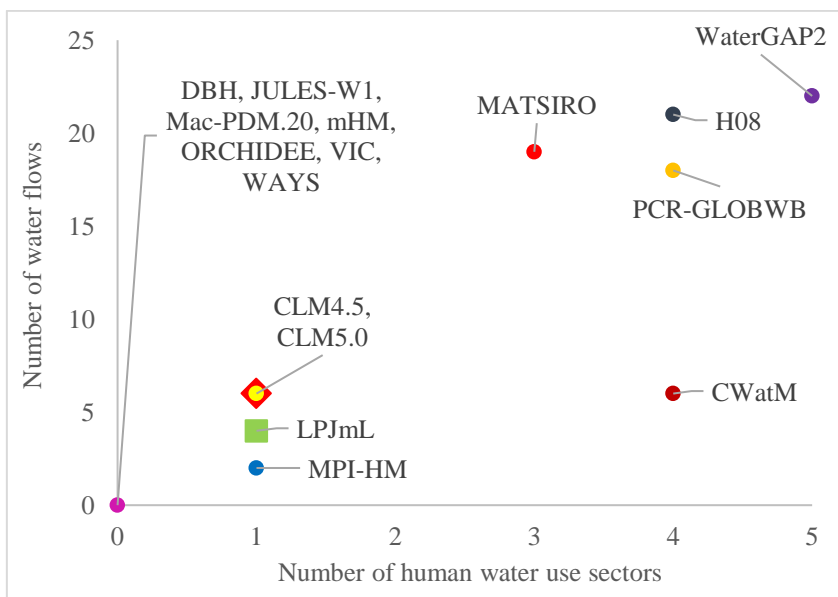
Figure 4: Number of human water use sectors and related water flows included in the global water models.

Table 12: Code availability of the ISIMIP2b Global water models

Model Abbreviation	Code availability	References
CLM4.5	CLM4.5 is under active development by the University Corporation for Atmospheric Research (UCAR) - National Center for Atmospheric Research (NCAR; https://ncar.ucar.edu). The model version is licensed under CC BY 4.0. The exact version of the model, used to produce the results of this paper, is archived on Zenodo (Thiery, 2020).	Oleson and Lawrence, 2013
CLM5.0	CLM5.0 is under active development by the University Corporation for Atmospheric Research - National Center for Atmospheric Research and hosted at the National Center for Atmospheric Research (NCAR; https://ncar.ucar.edu/). The version of model is licensed under CC BY 4.0. The exact version of the model, used to produce the results of this paper, is archived on Zenodo (CTSM Development Team, 2020).	Lawrence et al., 2019
CWatM	CWatM is under active development funded by the International Institute for Applied Systems Analysis (IIASA, Austria; http://www.iiasa.ac.at/cwatm). CWatM is open source and available online via GNU General Public License v3. The code can be used on different platforms (Unix, Linux, Window, Mac) and is provided through a GitHub repository https://github.com/cwatm/cwatm. The version of the model used to produce the results in this paper are stored as version 1.04 in the GitHub repository (https://github.com/CWatM/CWatM.) and at Zenodo (Burek et al., 2019).	Burek et al., 2020 Burek et al., 2019
DBH	DBH is under active development funded by the Institute of Geographic Sciences and Natural Resources Research, Chinese Academy of Sciences, Beijing, China (http://english.igsnrr.cas.cn/). The exact version of the model (global version 1), used to produce the results of this paper, is not open source. It is only available by request to the editors / reviewers in charge of this paper.	Tang et al., 2006; Liu et al., 2016
H08	H08 is under active development by the National Institute for Environmental Studies, Japan (Japan; http://www.nies.go.jp/index-e.html; http://h08.nies.go.jp). H08 is open source and available online via http://h08.nies.go.jp. The version of model is licensed under the terms and conditions: https://h08.nies.go.jp/h08/files/licence_en.pdf. The version of model is licensed under CC BY 4.0. The exact version of the model (model version 20190101), used to produce the results of this paper, is archived on Zenodo (Hanasaki, 2020).	Hanasaki et al., 2006; Hanasaki et al., 2008a,b; Hanasaki et al., 2018.
JULES-W1	JULES (the Joint UK Land Environment Simulator) is a community land surface model under continuous development by a wide community of UK researchers, coordinated by UKMO and CEH. The exact version of the model (version 4.7) used in these simulations is available from the Met Office Science Repository Service (registration required) at https://code.metoffice.gov.uk/trac/jules. To access the code a freely available non-commercial research license is required (https://jules-lsm.github.io/).	Best et al., 2011; Clark et al., 2011
LPJmL	LPJmL is under active development funded by the Potsdam Institute for Climate Research (Germany; https://www.pik-potsdam.de/en/home). The exact version of the model (model version 3.5), used to produce the results of this paper, is not open source. It is only available by request to the editors / reviewers in charge of this paper.	Gerten, 2004; Bondeau et al., 2007; Rost et al., 2008; Biemans et al., 2011
Mac-PDM.20	Mac-PDM.20 is under active development by the University of Nottingham (UK; https://www.nottingham.ac.uk/) and the University of Reading (UK; https://www.reading.ac.uk/). The version of the model (version 20), used in ISIMIP2b and in this paper, is not open source as it under active development. It is only available by request to the editors / reviewers in charge of this paper.	Gosling and Arnell, 2011; Smith, 2016
MATSIRO	MATSIRO is under active development funded by the University of Tokyo (Japan; https://www.u-tokyo.ac.jp/en/index.html) and National Institute for Environmental Studies (Japan; http://www.nies.go.jp/index-e.html). The exact version of the model (model version MIROC-INTEG1), used to produce the results of this paper, is not open source. It is only available by request to the editors / reviewers in charge of this paper.	Takata et al., 2003; Pokhrel et al., 2012; 2015
mHM	mHM is under active development funded by the Helmholtz Centre for Environmental Research – UFZ (Germany; https://www.ufz.de/index.php?en=33573; https://git.ufz.de/mhm). The version of model is licensed under GNU General Public License v3: https://git.ufz.de/mhm/mhm/-/blob/develop/LICENSE. The exact version of the model (model version 5.10), used to produce the results of this paper, is archived on Zenodo (Samaniego et al., 2017).	Samaniego, 2017 ; Samaniego et al., 2010; Kumar et al., 2013; Thober et al., 2019
MPI-HM	MPI-HM was developed at the Max Planck Institute for Meteorology (Germany; https://mpimet.mpg.de/en/homepage). The exact version of the model (model version 1.2), used to produce the results of this paper, is not open source. It is only available by request to the editors / reviewers in charge of this paper.	Stacke and Hagemann, 2012
ORCHIDEE	ORCHIDEE is under active development funded by the Institute Pierre Simon Laplace (France; https://www.ipsl.fr/en/; http://forge.ipsl.jussieu.fr/orchidee/wiki/Branches/ORCHIDEE-MICT-	Guimberteau et al., 2014; Guimberteau et al., 2018

	IMBALANCE-P/MergeNews). The source code for ORCHIDEE- MICT version 8.4.1 is available online, but its access is restricted. Consequently, one is required to communicate with the corresponding author for a username and password. The source code can be found at the following address: https://forge.ipsl.jussieu.fr/orchidee/browser/branches/ ORCHIDEE-MICT/tags/ORCHIDEE_MICT_8.4.1 The exact version of the model (model version v8.4.1), used to produce the results of this paper, is not open source. It is only available by request to the editors / reviewers in charge of this paper.	
PCR-GLOBWB	PCR-GLOBWB is under active development funded by the Utrecht University (The Netherlands; https://www.uu.nl/en/research/department-of-physical-geography). PCR-GLOBWB is open source and available online via: https://github.com/UU-Hydro/PCR-GLOBWB_model.The version of model is licensed under GNU General Public License v3. The exact version of the model (model version 2.0), used to produce the results of this paper, is archived on Zenodo: https://doi.org/10.5281/zenodo.1045338 (Sutanudjaja et al., 2017).	Van Beek et al., 2011; Wada et al., 2011; Wada et al., 2014; Sutanudjaja et al., 2018
VIC	VIC is under active development funded by the University of Washington, (USA; https://vic.readthedocs.io/en/master/). It was applied by the Indian Institute of Technology Gandhinagar, Gandhinagar (India; http://www.iitgn.ac.in/). VIC is open source and available online via https://github.com/UW-Hydro/VIC. The version of model is licensed under GNU General Public License v2.0. The exact version of the model (model version 4.1.2.g), used to produce the results of this paper, is archived on Zenodo (Shah and Vimal, 2020).	Gao et al., 2009
WaterGAP2	WaterGAP2 is under active development funded by the Goethe University Frankfurt (https://www.goethe-university-frankfurt.de/en?legacy_request=1; https://www.uni-frankfurt.de/45218063/WaterGAP) and Kassel University (https://www.uni-kassel.de/uni/) (Germany). The exact version of the model (model version 2.2c), used to produce the results of this paper, is not open source due to licensing issues. It is only available by request to the editors / reviewers.	Döll et al., 2012, 2014; Portmann et al., 2010; Müller Schmied et al., 2014, 2016; Verzano et al., 2012; Flörke et al., 2013
WAYS	WAYS is under active development funded by the Southern University of Science and Technology – SUSTech (China: https://www.sustech.edu.cn). The version of model is licensed under Creative Commons Attribution 4.0 International. The exact version of the model used to produce the results used in this paper is archived on Zenodo (Mao and Liu, 2019).	Mao and Liu, 2019